Universitat de Girona

Roberto Jorge Martínez Padilla

Experimental characterisation of the damping coefficient for composite materials

FRP++
Advanced structural analysis and design using composite materials

Master Dissertation
European Master Advanced Structural Analysis and Design using Composite Materials

Work developed under the supervision of
Doctor Daniel Trias Mansilla

Funded by the European Union

July 2026

DECLARATION

Name: Roberto Jorge Martínez Padilla

Email: robertomartinez.p@yahoo.com **Phone number:** +34 666 105131

Title of the Dissertation: Experimental characterisation of the damping coefficient for composite materials

Supervisors:

Doctor Daniel Trias Mansilla

Year of Conclusion: 2026

Master Course in Advanced Structural Analysis and Design using Composite Materials

THE ENTIRE REPRODUCTION OF THIS DISSERTATION IS AUTHORIZED ONLY FOR RESEARCH PURPOSES, UPON WRITTEN DECLARATION BY THE INTERESTED PERSON, WHICH IS COMMITTED TO.

University of Girona, 15/07/2026

Signature: Roberto Jorge Martínez Padilla



ACKNOWLEDGEMENTS

I want to start thanking all of teaching and managing staff from the FRP++ Advanced Structural Analysis and Design using Composite Materials program. The work and effort they give every day, to deliver not only an interesting but mostly advanced master course, is so rewarded. With every class work, school visit to the field and amazing conferences with expert people. I am nothing but satisfied and happy to write these words on what is the culmination of the past year with courses and projects, and now finishing my final dissertation.

To the Universitat de Girona and my professor supervisor Daniel Trias, who gave me the opportunity to work on this interesting and challenging topic. The support and guidance through the entire project, as well as the tools and facilities to complete my research.

To my colleagues and friends, for all the coffee breaks, lunch time and after school activities. All this social and recreational activities were key to keep the focus and stay relaxed during studies and hard-working times.

Finally, I want to thank my parents and family who have given me all the tools and education possible to be right here at this moment. Combined with all the effort I dedicate on pursuing my professional career; Now I can say I'm a Master graduate and I share and celebrate with them this incredible milestone of my life.

Caracterización experimental del coeficiente de amortiguación para materiales compuestos

RESUMEN

Los materiales compuestos se utilizan con frecuencia en diferentes sectores industriales. Específicamente, debido a su excelente relación resistencia/masa y rigidez/masa, estos materiales representan una opción ideal para estructuras de gran tamaño, como las palas de los aerogeneradores. Con el objetivo de mejorar la reciclabilidad de los materiales utilizados en la producción actual, es necesario un estudio de caracterización de los materiales para validar la sustitución de una matriz termoestable por una termoplástica, así como la introducción de fibras de origen natural. Para ello, es necesario determinar las propiedades mecánicas habituales pero también las propiedades dinámicas, como el coeficiente de amortiguación que está directamente relacionado con la vida útil y el mantenimiento de los componentes mecánicos. Por este motivo, y dada la falta de procedimientos y normas certificadas para calcular el coeficiente de amortiguación de un material compuesto, el objetivo de esta tesis es identificar y establecer las mejores prácticas para caracterizar adecuadamente dicho coeficiente en materiales polímeros reforzados. En primer lugar, se diseñó un componente de fijación mecánica para el montaje experimental, mismo que se validó mediante análisis de elementos finitos. Se probaron diferentes tipos de excitaciones, así como diferentes posiciones del acelerómetro, con el fin de encontrar la mejor configuración de ensayo para obtener datos experimentales. Asimismo, se presentan diferentes métodos de cálculo del coeficiente de amortiguación propuestos por distintos autores y se comparan los resultados de los distintos enfoques. Los resultados finales mostraron que el ancho de banda de media potencia, junto con un análisis de zoom en las bajas frecuencias, es el mejor método para obtener valores fiables con un bajo coeficiente de variación. Los valores del coeficiente de amortiguación obtenidos mantienen la correlación con los valores de diferentes materiales presentados por distintos autores.

PALABRAS CLAVE: Coeficiente de amortiguación; Caracterización dinámica; Ancho de banda a media potencia; Señales de excitación; Vibraciones en materiales compuestos.

Caracterització experimental del coeficient d'amortiment per a materials compostos

RESUM

Els materials compostos s'utilitzen cada cop més en indústries més diverses. A causa de la gran relació resistència/masa i rigidesa/masa, aquests materials són una opció excel·lent per a grans estructures com les pales d'aerogeneradors eòlics. Amb l'objectiu de millorar la reciclabilitat dels materials de la producció actual, cal un estudi de caracterització de materials per verificar la substitució d'una matriu termoestable per una termoplàstica, així com l'ús de fibres d'origen natural. Amb aquesta fi és necessari determinar les propietats mecàniques habituals però també les propietats dinàmiques, com el coeficient d'esmorteïment, que té una relació directa amb la vida útil i el manteniment dels components mecànics. Per aquest motiu, i a causa de la manca de procediments i normes certificadess per a calcular les propietats d'esmorteiment d'un material compost, l'objectiu d'aquesta tesi és trobar i establir les millors pràctiques per caracteritzar correctament aquest coeficient en el cas d'un material polímer reforçat amb fibres. En primer lloc, s'ha dissenyat un suport mecànic per a la configuració de l'experiment, validat mitjançant anàlisi per elements finits. Es van provar diferents tipus d'excitacions, així com diferents posicions d'acceleròmetres, per trobar la millor configuració d'assaig per obtenir dades experimentals. A més, diferents autors presenten diferents mètodes de càlcul per al coeficient i es comparen els resultats dels diferents enfocaments. Els resultats finals van mostrar que el mètode del mig ample de banda, amb l'ajuda d'una anàlisi de zoom a baixes freqüències, és el millor mètode per obtenir valors fiables amb un coeficient de variació baix. Els valors del coeficient d'esmorteïment obtinguts mantenen la correlació amb els valors de diferents materials presentats per diferents autors.

PARAULES CLAU: Coeficient d'esmorteïment; Caracterització dinàmica; mig ample de banda; Senyals d'excitació; Vibració en materials compostos.

Experimental characterisation of the damping coefficient for composite materials

ABSTRACT

Composite materials have become essential in numerous engineering sectors due to their outstanding mechanical performance. Specifically, due to the great strength/mass and stiffness/mass ratio, these materials represent an ideal option for big structures like aerogenerator wind blades. Aiming to improve the material recyclability of the current production, a study on material characterization is required to approve the substitution of a thermoset by a thermoplastic matrix, as well as the introduction of natural fibers. In consequence, it is required to determine not only the usual mechanical properties but also the dynamic ones, like the damping coefficient, which is in fact strongly related to the service life and maintenance of mechanical components. For this reason, and because of the lack on certified procedures and norms to compute the damping properties of a composite material, the objective of this dissertation is to find and stablish best practices to properly characterize dynamic coefficient for fiber reinforced polymers. First a mechanical attachment was designed for the experiment setting. Validated with finite element analysis. Different types of excitations, as well as different accelerometer positions were tested for finding the best test configuration to obtain experimental data. Also, different damping method calculation are presented by different authors and results are compared for different approaches. Final results showed half-power bandwidth aided by a zoom analysis on low frequencies are the best method to obtain reliable values with low coefficient of variation. The damping coefficient values founded keep the correlation with values from different materials presented by different authors.

KEYWORDS: Damping coefficient; Dynamic characterization; Half-power bandwidth; Excitation signals; Vibration in composites.

TABLE OF CONTENTS

Acknowledgements III
Resumen IV
Resum V
Abstract VI
Table of Contents VII
List of Figures IX
List of Tables XI
List of Abbreviations and Symbols XII
1. Introduction 1
1.1. Motivation 1
1.2. Objectives 2
1.3. Structure of the dissertation 3
2. Literature Review 5
2.1. Damping and modal analysis 5
2.2. Past and current research 7
2.3. Damping in Composites 8
2.4. Research gaps 10
3. Methodology 11
3.1. Experiment configuration 11
3.2. Pre-Analysis 13
3.2.1. Analytical approach 13
3.2.2. Finite Element model 14
3.2.3. Attachment design 16
3.3. Test variables 17
3.3.1. Type of excitation 17
3.3.2. Accelerometer/Sensor 19
3.4. Damping Calculation 22
3.4.1. Zoom Analysis 23

3.4.2. Reverberation Time 24
4. Results and Discussion 27
4.1. Natural Frequencies 27
4.2. Damping Coefficient 29
4.2.1. Statistical analysis 32
4.3. Modal shapes 34
5. Conclusion 37
5.1. Main Conclusions 37
5.2. Further developments 38
6. References 39
Appendix I: Mechanical attachment 41
Appendix II: Finite Element analysis 43
Appendix III: Samples FRF 51
Appendix IV: Modal shapes 55

LIST OF FIGURES

Figure 2.1-1: 3dB-bandwidth method schematic [4] 6
Figure 2.2-1: Comparison on different excitation waveforms [8] 7
Figure 2.3-1:Comparison of loss factor with different material fibre orientations [10] 10
Figure 3.1-1: Schematic of test configuration devices 11
Figure 3.1-2:(a) Attachment design (CAD render) (b) Clamp part design (CAD render) 13
Figure 3.2-1: ABAQUS model for a composite probe 15
Figure 3.2-2: First modal shape of assembly with attachment included 17
Figure 3.3-1: Comparison on different input signals for same probe material 18
Figure 3.3-2: Fourth modal shape of a composite sample 21
Figure 3.4-1: Sample (*S_G45_Si*) first mode damping factor 23
Figure 3.4-2: Zoom analysis, Sample (*S_G45_Si*) first mode damping factor 24
Figure 3.4-3: IRF for sample (*S_G45_Si*) for the first mode 25
Figure 4.1-1: Frequency Response Function (FRF) of sample (*S_G45_Si*) 28
Figure 4.2-1: Data from the Table 4.2-3 31
Figure 4.3-1: First modal shape obtained by experimental testing 34
Figure 4.3-2: First modal shape obtained by FE model 35
Figure A.I - 1: Technical Drawing of mechanical attachment 41
Figure A.I - 2:Technical Drawing of clamp attachment 42
Figure A.II - 1: Probe *S_G45_Si* first vibration mode (28 Hz) 43
Figure A.II - 2: Probe *S_G45_Si* second vibration mode (173 Hz) 43
Figure A.II - 3: Probe *S_G45_Si* third vibration mode (485 Hz) 44
Figure A.II - 4: Probe *S_G45_Si* fourth vibration mode (947 Hz) 44
Figure A.II - 5: Probe *S_G45_Si* fifth vibration mode (1560 Hz) 45
Figure A.II - 6: Assembly *S_G45_Si* first vibration mode (28 Hz) 45
Figure A.II - 7: Assembly S_G45_Si second vibration mode (176 Hz) 46
Figure A.II - 8: Assembly *S_G45_Si* third vibration mode (494 Hz) 46
Figure A.II - 9: Assembly *S_G45_Si* fourth vibration mode (969 Hz) 47
Figure A.II - 10: Assembly *S_G45_Si* fifth vibration mode (1608 Hz) 47
Figure A.II - 11: Mesh of the probe, zoom in picture to clearly see the squares (avg. aspect ratio = 1.0) 48

Figure A.II - 12: Mesh of mechanical attachment (avg. aspect ratio = 1.8)..... 48
Figure A.II - 13: Mesh of clamp attachment (avg. aspect ratio = 1.6) 49
Figure A.II - 14: Flax characteristic values used in ABAQUS 49
Figure A.II - 15: Boundary conditions in assembly model 50
Figure A.II - 16: Interactions in assembly model 50
Figure A.III - 1: Frequency Response Function for S_G00_Si..... 51
Figure A.III - 2: Frequency Response Function for S_G00_Ak 51
Figure A.III - 3: Frequency Response Function for S_G45_Si..... 52
Figure A.III - 4: Frequency Response Function for S_G45_Ak 52
Figure A.III - 5: Frequency Response Function for S_F00_Si 53
Figure A.IV - 1: Experimental test first modal shape for S1_G45_Ak..... 55
Figure A.IV - 2: Experimental test second modal shape for S1_G45_Ak..... 55
Figure A.IV - 3: Experimental test third modal shape for S1_G45_Ak 56
Figure A.IV - 4: Experimental test fourth modal shape for S1_G45_Ak 56
Figure A.IV - 5: Experimental test fifth modal shape for S1_G45_Ak..... 57

LIST OF TABLES

Table 3.1-1: Different samples characteristic data 12

Table 3.2-1: Unidirectional (Glass fibre + Sicomin) composite characteristic values 15

Table 3.2-2:Comparison of natural frequencies [Hz] for different methods 16

Table 3.3-1: [S_G45_Ak] Natural Frequencies in [Hz] for different accelerometer positions. 19

Table 3.3-2: Distances with zero displacement for each mode 20

Table 3.3-3: Damping coefficient for same probe but different accelerometer positions 21

Table 4.1-1: Natural frequencies for first five modal modes for each sample 27

Table 4.1-2: Comparison on different bandwidth studies for sample (*S_G00_Si*) 29

Table 4.2-1: Damping coefficient [ζ] with reverberation time method 29

Table 4.2-2: Damping coefficient [ζ] with half-power bandwidth method 30

Table 4.2-3: Damping coefficient [ζ] with mixed methods 30

Table 4.2-4: Nat. freq. and damping coeff. for (S_G45_Ak) samples with half-power bandwidth method 32

Table 4.2-5: Nat. freq. and damping coeff. for (S_G45_Ak) samples with reverberation time method 33

Table 4.2-6: Mean damping coefficient [ζ] excluding first mode 33

LIST OF ABBREVIATIONS AND SYMBOLS

Abbreviations

PLA	Polylactic acid
FEA	Finite Element Analysis
FRF	Frequency Response Function
B&K	Brüel & Kjaer
CAD	Computer Aided Design
DOF	Degree of freedom
FE	Finite Element
IRF	Impulse Response Function
CoV	Coefficient of variation

Symbols

δ	damping factor
f_0	Natural frequency
η	Loss factor
ζ	Damping ratio or damping coefficient
α_n	End condition constant
L	Length of beam
I	Second moment of inertia
A	Cross-sectional area
ρ	Density
n	Modal mode
E	Modulus of elasticity
E_x	Modulus of elasticity in longitudinal direction
t	Plat thickness
A_{ij}	Terms from the laminate stiffness matrix
X_n	Accelerometer distance from fixed end
σ	Decay rate
τ	Time constant

1. INTRODUCTION

In this first section the motivation and main objectives of the present dissertation are introduced.

1.1. Motivation

In the last decades composite materials use on different industries has grown exponentially becoming more and more a common choice among designers for different structures [1]. They are well known for having very good mechanical properties while keeping a low weight. The high strength-to-weight ratio makes composites a great material choice to be used as reinforcement structures and in complex industries that require enhanced performance. Aeronautic, energy, civil engineering, automotive and naval are some examples of sectors where composites are mostly used.

In short, composites are a combination of two or more materials merged together, usually identified as fibre or reinforcement, the one who will carry the most of the loading, and matrix, working as a joining for the different components. Consequently, the final characteristic values and properties obtained for each material will differ from one another. One example of these differences relies on the damping behaviour of the composite, which is a relevant characteristic to take into account when designing a structure subject to dynamic loading. High damping coefficients may help in reducing the amplitude of vibrations and consequently maintenance of components and their fatigue life. [2]

Engineering design is all about creating new parts and assemblies that will work together in machinery performing a job. This work is constantly a loop process, where improving and finding better solutions are always present. In the case with composite materials, changing the manufacturing variables to get the desired performance is a common challenge engineers face every redesign stage. Bhudolia states [3] that, going from a thermoset to thermoplastic in a composite may improve the damping response of a material. Therefore, the interest in having a procedure test, engineers in academia and industry can follow to compare these minor changes on different material production.

The dissertation itself comes from a past project done at the Universitat de Girona called SUCCESBLADE, where different values of damping were requested in an effort to substitute the matrix for a current production wind generator blade. There was uncertainty on the work done in the AMADE research group, since it showed values of different order of magnitude to those published for similar materials, particularly for low frequencies. Also, the lack of details in norms and regulations for the testing could have affected the results obtained. For this first experimental testing a 3D (PLA[1]) machined attachment was used to fix the material probes to the shaker system. There was doubt on the inherence of the attachment to absorb some energy during the vibrations. No finite element analysis or computer software was used to validate the correct modal analysis and damping study. Therefore, the interest on performing the experimental testing again.

1.2. Objectives

Usually for material characterization, tests with norms and experimental parameters are followed. The regulations and specifications for testing are well documented in order to obtain trustworthy values. Unfortunately, in the case of the damping coefficient for composites, the lack on certified procedures makes it difficult to compute and get reliable values. Important to mention the wide number of variables (type of excitation, type of sensor, position, physical attachment, etc.) that can be changed and used when performing experimental testing.

The main objective of this thesis is to define and come up with a technique that can be used to test and further on compare different damping ratios for composite materials. This includes finding the best test variables that can suit the experimental testing, design and validate a robust attachment that can be used on the test configuration, and finally correlate the data obtained with the one computed with Finite Element Analysis (FEA).

[11] Polylactic acid or polylactide (PLA), is a thermoplastic polyester

The materials to be compared in this project are the same ones available from the past project resources (SUCCESBLADE), and the principal outcome of this thesis will focus on getting a procedure to test materials, that could be further used by any other interested means to test composite materials as desired.

1.3. Structure of the dissertation

The thesis will start with a literature review exposing some of the research done so far in the topic, giving the reader some insight on how different variables may change the damping coefficient of a composite. Also sharing test performed in the past by different researchers and how were the experimental results to further compare with the ones obtained in this project. Next the methodology and structure will be presented, where specifications and deep detail on variables chosen will be discussed. In Section 4 the results are given to finally write some conclusions in the fifth section.

THIS PAGE WAS INTENTIONALLY LEFT BLANK

2. LITERATURE REVIEW

Before developing a methodology for the experimental characterization of the damping coefficient in composite materials, this section presents the most relevant research works performed in the topic: first general information about experimental modal analysis and the relevance in mechanical engineering, next recommendations and the current research done to estimate damping in composite materials, after then a more detailed information on how composites behave with respect to damping behaviour, and finally some research gaps and considerations to take into account on the topic.

2.1. Damping and modal analysis

Vibrations and noise (representation of unwanted vibration through air) are the result of some excitation force and the dynamic response (through time) of the structure and/or a material in question. For mechanical engineers the unwanted vibrations represent discomfort or annoyance, reduced lifetime of a component/machine and mostly important, hazardous situations for a part or person operating machinery. Damping refers in this case as the action to absorb energy on a system and dissipate it by means of temperature, at most of the times. One of the most common examples of damping devices are the shock absorbers in mostly all of the road vehicles. With these components the vehicles can ride on bumpy streets without affecting the comfort of the passengers and maintaining the control while driving.

In mechanical structures for example, damping coefficient of a material is considered to know how the parts will respond to acting loads. With this in mind designers can consider the material characteristics and aim for a reduction in vibrations, helping to overcome fatigue in components and finally the extended life of the complete structure, not forgetting the reduction in cost and maintenance it also symbolizes.

Most of the vibrations and noises comes from some precise moments, exactly when a structure is at its peak point of response, also called resonance points which consequently are associated in mechanical engineering with the alleged modal modes. The modal analysis of a structure consists on getting the modal frequency, damping and shape of the assembly in question.

Research on different approaches to get experimentally the damping coefficient was done. One of the commonly mentioned methods among different authors is known as the half-power bandwidth method. From the frequency response function (FRF) damping factor could be obtained by identifying the peak resonance frequencies, which subsequently correspond to the natural frequencies or resonance modes of the specimen. After locating the different frequency resonances, the 3-dB bandwidth method is used to compute the damping coefficient of the material, at the desired modal point. In Figure 2.1-1 a schematic of FRF graph is shown, also the values needed from it to compute the damping factor.

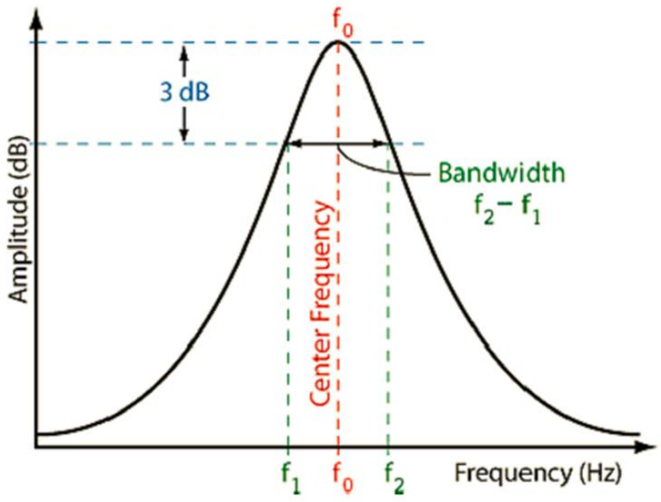


Figure 2.1-1: 3dB-bandwidth method schematic [4]

The Eq. (2.1-1) shows how to obtain the damping factor (δ) with f_0 the natural frequency in Hz of the mode in analysis, and f_1 and f_2 are the frequencies, also in Hz, at which from the FRF the amplitude is 3 dB lower before and after the resonance frequency (f_0). This difference is also known as the bandwidth. Represented in Eq. (2.1-2) the loss factor (η) is also another way to refer the damping coefficient but with different term and calculation. Here the symbol (ζ) represents the damping ratio (or damping coefficient).

$$\delta = \frac{f_0}{\Delta f} = \frac{f_0}{f_2 - f_1} \tag{2.1-1}$$

$$\eta = \frac{1}{\delta} = 2 \cdot \zeta \tag{2.1-2}$$

2.2. Past and current research

Many approaches have been done in researching to get experimental values for damping coefficient in composites [5], [6]. Some examples of different test configurations done in the past can be seen on research done by Treviso, A. [1] . In comparison with alloys, where different specimen and test variables deliver a linear response on the damping ratio [7], materials like composites may behave quite differently when distinct test parameters are taken. From these variables type of excitation and sensors used are the most common ones to change among experiments.

Random, Pseudo Random, Periodic Random, Sine Swept, Burst Random are examples of type of excitations available within the experimental configuration. As mentioned by the instrument supplier [8], the differences mainly rely on computation time and possible error found (noise, leakage error) on the recording of the response signal. For modal testing using a shaker, it is generally recommended to avoid some excitation waveforms, like Sine Swept [9]. More detailed information on advantages and disadvantages of different input signals can be found on Figure 2.2-1.

Waveform	Analysis Speed	Leakage Error ?	Linear Approximation ?	Crest Factor S/N Ratio	Spectrum Control	Zoom Analysis ?	χ^2-detects non-linearities ?	χ^2-detects leakage ?
Sinusoidal	very slow	yes	no	good	high	yes	no	no
Random	slow	yes	yes	fair	high	yes	yes	yes
Pseudo Random	fast	no	no	fair	high	yes	no	no
Impact	fastest	no (with exp. window)	no	poor	limited	no	no	no
Multiple Impact	slow	yes	some	poor-fair	limited	no	(yes)	yes

Figure 2.2-1: Comparison on different excitation waveforms [8]

For sensors the main two categories are contact and contactless sensors. From the first ones it is learned that lightweight transducers preferable should be used, to avoid adding mass to the sample, hence changing the material natural frequencies, consequently the damping coefficient computed. According to the instrument supplier Brüel & Kjaer (B&K) literature [8], less than 3% of the total mass should be accounted for the accelerometer in the testing sample. As second alternative sensors like the ones used by Berthelot [10] and Kayaaslan [11], could deliver a good work measuring the displacement of a probe without interfering on the material mass, obtaining values of damping coefficient around (0.65-0.75) % for glass fibre composites with 45^{o} fibre orientation. In comparison, Bhudolia [3] using mounted accelerometers found for carbon cross ply with thermoplastics values rounding (1.35-1.65) % as damping ratio.

2.3. Damping in Composites

In comparison with homogenous materials where different miscible materials have all the properties distributed equally along its volume, composite are highly dependent on the composition and manufacturing variables that are chosen while production. Damping coefficient can be therefore quite distinct from conventional materials like metals and alloys and, unlike most static mechanical properties, cannot be approximated by physically based equations based on the properties of the constituents

Five main sources of energy dissipation are presented by Chandra [12]. (a) For start the viscoelastic composition of the matrix but also in some cases by the fibres. In composites the major contributor to damping is the matrix used on the material. (b) Second comes damping caused by the interphase, which in case of composites refer to the region surrounding the fibres across its length. (c) The different failure modes mechanisms distinguish composites from other materials being damping due to damage as the third main cause. Examples of energy dissipation can be found due to matrix cracks, fibre breakage, delamination, etc. (d) The intended use of the material within its elastic limit also should be considered when obtaining the damping coefficient, since large amplitudes or high stress levels can induce the non-elastic damping behaviour, especially with thermoplastics matrices. (e) Finally, the

temperature and the effect it has on the response of a material. When vibrations occur, cyclic load is transferred between the compressive and the tensile region of a composite, which may rise significantly the temperature of a thermoplastic [13] and therefore the effective energy dissipation exhibited by the material.

Focusing on the matrix it is important to make the distinction between the different polymers used on the market. During the last decade more and more emphasis on replacing thermosets with thermoplastics has been on research. Primary due to the environmental impact and the good recycling options thermoplastics offer. Nonetheless mechanical properties may be on disadvantage when compared with thermosets [14]. On the other hand, thermoplastics exhibit better performance to impact damage, releasing and dissipating better the energy [11]. Hence the need on testing different material configurations that will lead to a good compromise between stiffness and damping behaviour. In the research done by Duc [14] the theoretical expected result of thermoplastics having an increased damping coefficient is discussed with the experimental results.

Other variables that affect the damping response on composites is the fibre orientation and the fibre volume [10]. Both of them play a huge role when designing a new material. For fibre orientation it is proven that 0^o oriented composites will have lower damping ratio as a 45^o for example Figure 2.3-1. This mainly due to the load and work done by the matrix, which is the main contributor to energy dissipation. Same reason applies for the fibre content, where less fibre volume are more matrix or other nanomaterials (e.g., adhesives) would be, therefore an increase in damping coefficient is expected.

From [4] was learned that adding different material reinforcements can led to an improvement on damping ratio. In this study composite plies of carbon were added to a unidirectional flux laminate, in this case to obtain similar damping coefficient but with increased strength of the material. Also, different ply stack-up configuration was studied by moving a flux cross-ply ($+/-45^o$) from top layer to the inside of the laminate. From this research damping ratios of flux fibre with added carbon layers are around (0.18-0.24) % for the second mode of vibration. Emphasis on the modal mode is mentioned, since different modal modes can deliver different mechanisms on the materials because of the frequency at which the material oscillates [4].

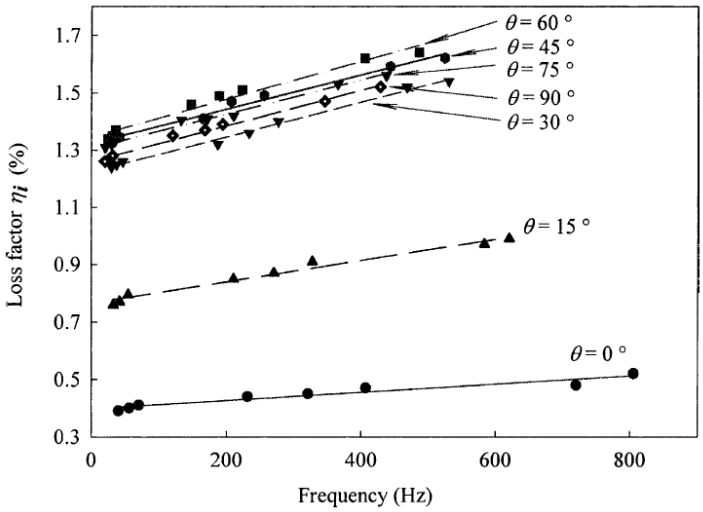


Figure 2.3-1:Comparison of loss factor with different material fibre orientations [10]

2.4. Research gaps

The lack of norms and standardized test regulations makes the experimental approach a carefully process to follow. Conditions like air damping and contact-less measurement should be considered to obtain better results on the study. Nonetheless for matter of this project, the test configuration will take into consideration the most possible advices found on literature to follow during experimental research. Recommendations and specifications of the norm ISO 6721-1 was adopted, since it applies to polymers, which is mostly similar to composite materials. However, the norm does not specify some of the parameters of the test which might have a decisive influence on the measurement.

3. METHODOLOGY

The methodology followed will be explained in this section. Starting with the experiment configuration, material and devices used; next some explanation on support analysis done prior the experimental testing; then the test variables will be discussed and why they were chosen; and finally, the different ways to calculate the damping coefficient will be presented.

3.1. Experiment configuration

For the experimental test all devices and instruments used are from the same supplier company (B&K). A schematic of the configuration can be seen in Figure 3.1-1. An Electrodynamic Shaker B&K V406-LDS will perform the vibration for the testing. B&K Accelerometers 4508-1 and 4517 are connected to the Acquisition Module B&K LAN-XI, together these devices will record the material response from the excitation signal. To enhance the input profile an amplifier V406-LPA100 is connected between the computer and the shaker device. For processing, test configuration and visualization of all data, Software B&K Connect© is used.

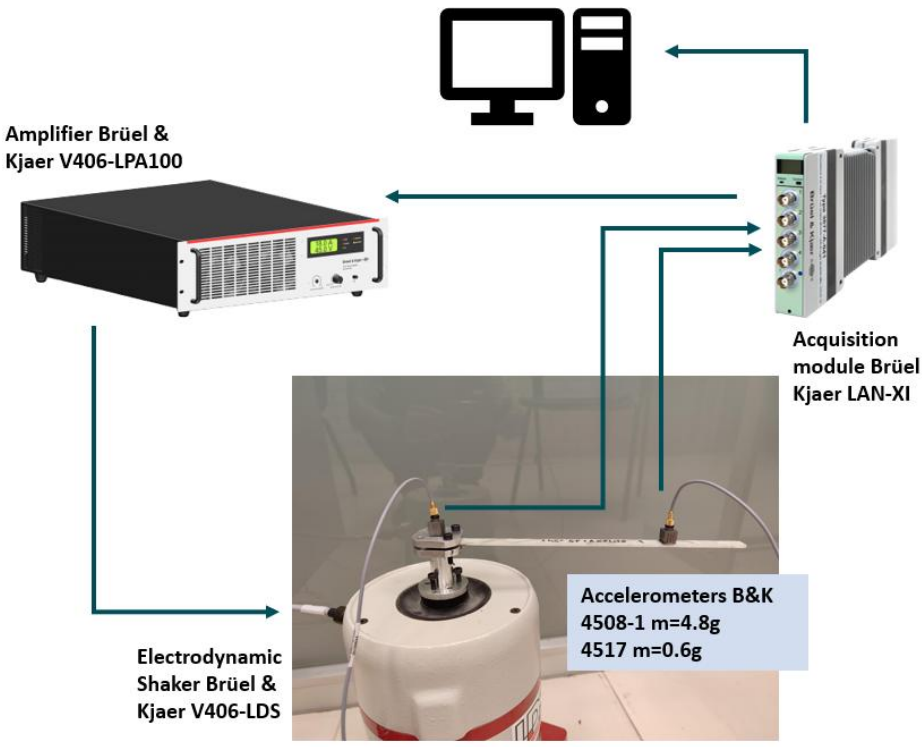


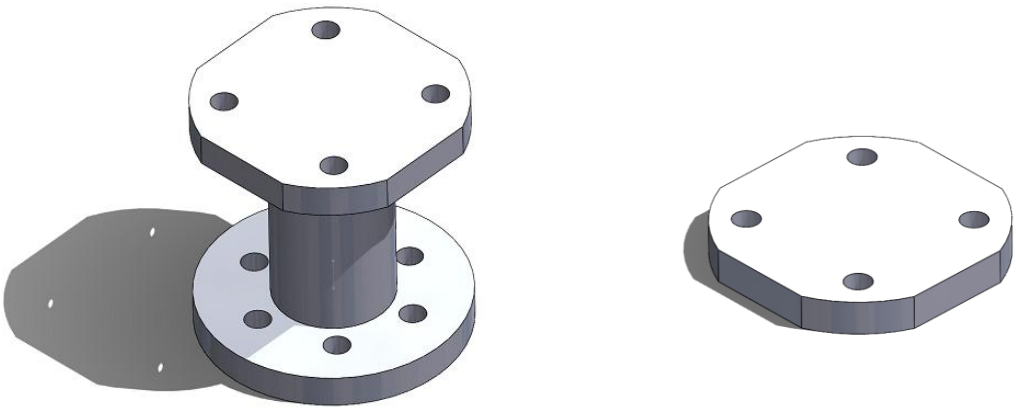
Figure 3.1-1: Schematic of test configuration devices

The different material configurations used in this project are presented in Table 3.1-1. Rectangular prism shape probes were chosen, first because the easy manufacturing of the samples, but also together with the support to simile a cantilever beam with simple geometry, easy to perform analytical analysis from it.

Table 3.1-1: Different samples characteristic data

Sample	Material	Thickness [mm]	Width [mm]	Length [mm]	Mass [g]
S_G00_Si	GF 8092 UD 0^o + Sicomin	1.1	10	280	6.4
S_G00_Ak	GF 8092 UD 0^o + Akelite	1.1	10	280	6.4
S_G45_Si	BXE600 1270 STD BIAX ±45 ^{o} + Sicomin	3.7	10	280	21.5
S_G45_Ak	BXE600 1270 STD BIAX ±45 ^{o} + Akelite	3.7	10	280	21.5
S_F00_Si	UD FLAX + Sicomin	1.2	10	205	3.2

To properly fix the probes to the shaker an attachment component was designed. This part needed to be stiff enough not to alter the vibration response on the samples, but also it had to be small and light so the shaker device could efficiently transmit the excitation signal to the whole probe. For this step different design proposals were discussed to finally come up with the one presented in Figure 3.1-2. A small (40x40mm) round shaped part, easy to manufacture locally at the university facilities. The design of the part was done using Computer Aided Design (CAD) software tool SOLIDWORKS©. Also, the material decided for this part was aluminium, since it has a lower density than steel but also is stiff enough to absorb the least mechanical vibrations from the saker to the composite. As the usual damping ratios for metals in elastic region are lower than 1%, which is 5 times less than the one expected for polymers [15]. A further detail on the part dimensions can be seen in Appendix I. Detailed modal analysis on this part is discussed in Section 3.2.3. Finally, to fix the samples to the attachment base, a clamp face part was separately created, together with screw bolts these parts will create the pressure needed to hold the samples.



(a) (b)

Figure 3.1-2:(a) Attachment design (CAD render) (b) Clamp part design (CAD render)

3.2. Pre-Analysis

As it is shown in Section 2 the experimental analysis on damping coefficient requires the identification of the natural frequencies of the parts and/or structures tested. Since for this case a cantilever beam approach was decided, a comparison between analytical with numerical prediction is possible. In the following sub-sections analytical approach using MATLAB© software as a tool is presented. Also, the numerical and more trustable approach using ABAQUS© program to perform a Finite Element Analysis (FEA) will be discussed and compared.

3.2.1. Analytical approach

MATLAB software was used to compute the different sample dimensions and material properties. With a code it is simple and fast to change the material variables and have a quick look on the natural frequencies expected for each sample. The method used to get the natural frequencies of a cantilever beam follow the Lagrange's Equation [2]. The main formula is presented in Eq. (3.2-1) where α_n represents the constant of end condition for a cantilever beam, L is the length of the beam, I the second moment of inertia, A the cross-sectional area and ρ the density of the composite. The subindex (n) in this case represents the modal mode

order. For matter of this project the mode orders will be limit to the five first modes founded for a cantilever beam.

$$f_n = \left(\frac{\alpha_n^2}{2\pi L^2}\right) \sqrt{\left(\frac{EI}{\rho A}\right)} \tag{3.2-1}$$

Composite materials have direction-oriented properties, so for the Eq. (3.2-1) the equivalent modulus of elasticity (*E*) in longitudinal direction along the beam (E_x) needed to be computed [4]. For that the constitutive laminate theory was followed. With this method the elastic modulus can be obtained from Eq. (3.2-2) where terms A_{ij} are obtained from the laminate stiffness matrix and *t* represents the thickness of the laminate.

$$E_x = \frac{A_{11} * A_{22} - A_{12}^2}{t * A_{22}} \tag{3.2-2}$$

3.2.2. Finite Element model

To validate and have more accuracy than the analytical method (1st approach) a simple model in ABAQUS was created (2nd approach). Initially a model of just the composite probe alone was simulated. Composite layup section was created with the characteristic values of the material to test (See Table 3.2-1). One end of the beam was fixed and the other was left with free motion. Also, the two edges parallel to the longitudinal direction had applied boundary condition, in this case transverse axis (Y) remained constrained with zero displacement, as well as the rotation along the other two axis (X and Z). The main reason for this was to simulate the most similar condition as the experimental test will do (avoid torsion in model). Because the shaker only produces vibration in one direction, single degree-of-freedom (DOF) from the cantilever response was considered. In Figure 3.2-1 an overview of the model can be seen. For more details and images of the model in ABAQUS see Appendix II.

The step used in the simulation is [Linear Perturbation, Frequency]. Also, important to mention that simple shell square mesh 4-node (S4R) was used for this model (1.0mm length),

small enough to obtain the smooth displacements of the beam but also with a good and short computation time.

Table 3.2-1: Unidirectional (Glass fibre + Sicomin) composite characteristic values

Characteristic	Value
Density [g/cm^3]	1.83
E_{11} [GPa]	34.33
E_{22} [GPa]	4.81
E_{33} [GPa]	4.81
ν_{12} [-]	0.31
ν_{23} [-]	0.62
ν_{13} [-]	0.31
G_{12} [MPa]	3183.07
G_{23} [MPa]	2972.62
G_{13} [MPa]	3183.07

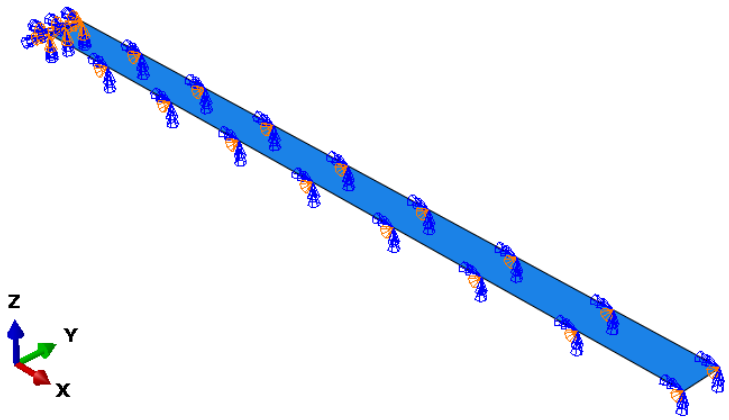


Figure 3.2-1: ABAQUS model for a composite probe

3.2.3. Attachment design

The attachment created and previously introduced in Section 3.1 was part from a design loop. To remember the reader, the main objective of this part is to create a support that will fix properly the probes to the shaker but also would not have effect on the measurement and damping response of the material tested.

At first the design was done using CAD tools. Then the part was exported to the FEA tool, to further on, together with the sample composite plates obtain the natural frequencies for the different modes. This is the modal analysis using Abaqus. The software would validate if the attachment was stiff enough to transmit the vibration without interfering the plate response. An image of the model can be seen on Figure 3.2-2. In Appendix II comparison of the first five modal shapes of the probe alone and the assembly with the probe is presented.

For this 3rd approach similar, but in different locations, boundary conditions were applied. The base of the attachment is fixed and longitudinal edges of the probe with symmetry. Additional interaction between the attachment and the clamp part was created to simulate the screw bolt fixing. For the step, same condition as 2nd approach. Because of more complex shapes the attachment and clamp had tetrahedral geometry mesh. The composite beam remains the same.

A comparative result on the natural frequencies obtained with, first the analytical method (MATLAB), second the simple mathematical method and third the assembly of all the components is presented on Table 3.2-2. It can be seen the three approaches deliver similar results being the analytical code a good quick tool to use for obtaining the order of magnitude of the natural frequencies of any sample. If more precision and detailed analysis is required, the ABAQUS model with all the components will be used.

Table 3.2-2:Comparison of natural frequencies [Hz] for different methods

Mode	1st MATLAB	2nd ABAQUS (probe only)	3rd ABAQUS (assembly)
1	29	28	28
2	180	173	176
3	503	485	494
4	986	947	969
5	1630	1560	1608

To further simile the condition of the experimental test, a 4th and final approach was computed with a mass inertia added to the model. This represents the mass of the accelerometer above the sample material. Because of the light weight of the sample, it is important to consider and take into account this component. Further discussion and comparison on results will be discussed in Section 4.

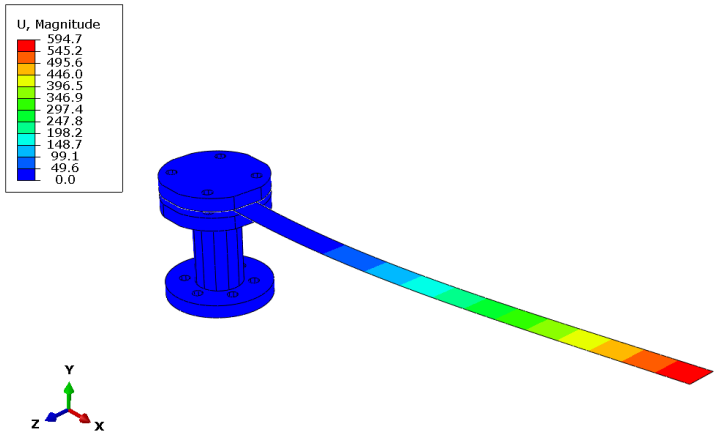


Figure 3.2-2: First modal shape of assembly with attachment included

3.3. Test variables

As shown in Section 2 many different variables and approaches can be taken to perform experimental testing with composites materials. From measurement devices, signal trigger and record, environmental conditions, all these elements play a big role on the value obtained after testing and consequently the parameters chosen should be consistent among different material probes.

3.3.1. Type of excitation

For a vibration test using a shaker, different input signals can be used to perform the excitation on the testing material. Excitation profile can be frequency centred oscillating at a specific ratio represented as a sine signal. Although for matter of this project a widespan of frequencies is preferred, since the different mode natural frequencies are required.

Different input signals were presented previously in Section 2.2 After testing and trying with different configurations, pseudo random excitation will be used to test the wide span spectra of the material. In Figure 3.3-1 it can be seen four different FRF graphs, each one representing different input signals for the same probe material (R: Random; PR: Pseudo Random; BR: Burst Random; PeR: Periodic Random). All the studies were performed for a 3.2kHz bandwidth.

From the results all of them deliver similar graph shape, clearly identifying the peak responses corresponding to the modal modes. Nonetheless the noise found in the blue and pink graph (BR and R) is quite more than the other functions. The other difference is computation time. For PR (red graph) the time taken was 33s to get 500 averages. For the PeR (green graph) the time to get 500 average data was around 2 minutes. Finally, all of the input signal testes deliver almost the same result, for example for the fifth mode the natural frequency was found in the frequency of 1460Hz and the damping coefficient computed rounded between (2.25-2.63) % for all the excitation types. Conclusion the fourth input signals are quite similar, is a matter of data quality recorded and time taken to get it.

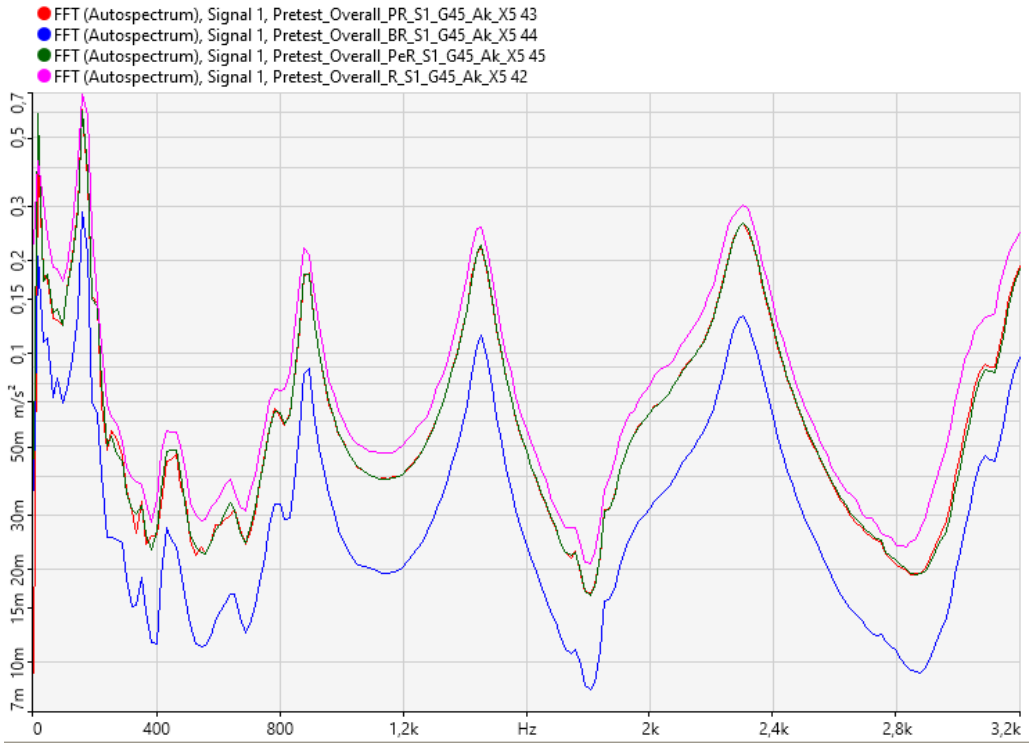


Figure 3.3-1: Comparison on different input signals for same probe material

3.3.2. Accelerometer/Sensor

Although contactless sensors are preferred for dynamic analysis, in this case mounting accelerometers will be used as described previously in Section 3.1. The accelerometers play a huge role on getting the correct data, mostly influenced by two factors, mass and position. Below different parameters will be discussed on the two testing variables.

Recalling Section 2.2 lightweight sensors should be employed, therefore the accelerometer 4517 (mass = 0.6g) would be used to attach to the probes. The other accelerometer 4508-1 (mass = 4.8g) is only used as reference from the whole system mounted directly on the upper part of the attachment. In this way measurement from the shaker and the testing sample can be compared.

Accelerometer position plays a big role on how accurate and noisy the response recorded will be. From literature read [8] it is advised to place sensors out of the nodal points or zones where displacement of the material tested is expected to be low or zero. Also, it is learned from other literatures [4] that high amplitude vibrations could alter the recording and give some noisy response which translates in an unclear peak response. Hence the importance on locating the accelerometer in a strategic position.

For this matter a study for a single sample [S_G45_Ak] with different accelerometer positions [X_1-X_5] was done. The distances X_n [n = 1-5] are the distances of the accelerometer from the fixed end of the sample. The results obtained are shown in Table 3.3-1. Here it can be seen for some positions the sensor is not capable of identifying (*NF*) the natural frequencies expected for the first five modes. Only the positions X_2 and X_5 identify all the peak resonances in the FRF.

Table 3.3-1: [S_G45_Ak] Natural Frequencies in [Hz] for different accelerometer positions

Mode	**Accelerometer position**				
	X_1 = 100 mm	X_2 = 120 mm	X_3 = 140 mm	X_4 = 160 mm	X_5 = 180 mm
1	32	32	16	16	16
2	144	160	176	NF	160
3	NF	464	448	464	464
4	880	896	NF	912	816
5	NF	1340	1260	NF	1380

NF = Not Found

To support the analysis and find weather the locations X_n of the sensor placed are the optimal, FE model simulation of Section 3.2.3 was used to identify at which distance from the fixed end the displacements are almost zero. Distances where displacement is negligible are presented in Table 3.3-2 for the different modal frequencies. For the first mode, all the area between the base of the fixed end (position = 0) to a distance of approximately 47mm from the base is considered to have low displacement. For other modes the base of the attachment is noted in the first column, but additional positions are mentioned. For example, for mode 3 it is expected negligible displacement at 105mm and 182mm from the fixed end of the sample. Note the strong correlation between the measurement capabilities of the experimental configuration with the expected zones of zero displacement. If we look at the measurement taken from testing, the third natural frequency was not found when the accelerometer was placed 100mm apart from the base, really near from the 105mm position noted in Table 3.3-2. Same apply for other modes at other distances.

Table 3.3-2: Distances with zero displacement for each mode

Mode	**Distances in [mm] from fixed end**				
1	0	<47.0			
2	0	174.0			
3	0	105.0	182.0		
4	0	75.0	135.0	185.0	
5	0	59.0	105.0	154.0	186.0

Also, an image of the mathematical model can be seen in Figure 3.3-2. where the blue colour represents the areas in which the displacement is zero and the red tones means the highest displacement. Note to consider, the displacements obtained from the model are just used as reference to find the areas where maximum and minimum are expected, not really for knowing how much the displacement would be.

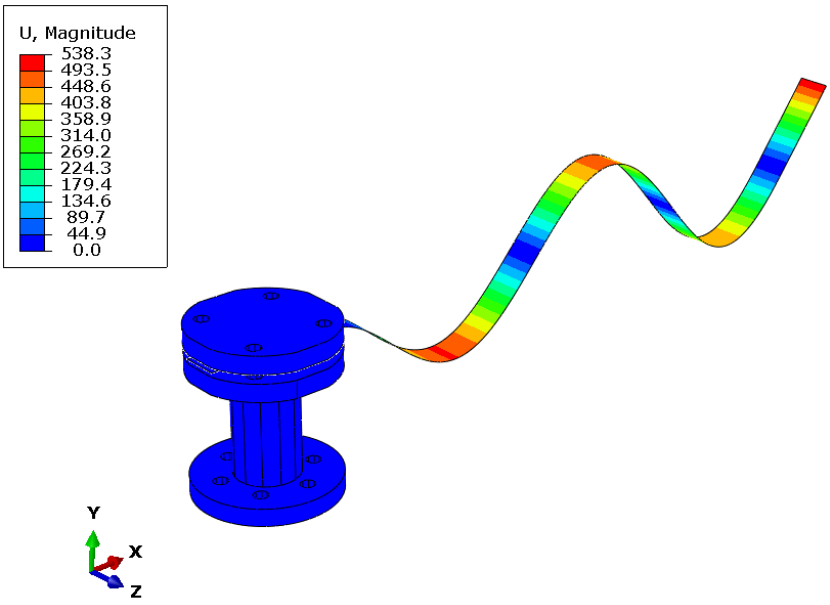


Figure 3.3-2: Fourth modal shape of a composite sample

After analysis and correlation from both the experimental testing and FE model data, the ideal position for the specifically probe samples with this geometry and material is around 120mm (X_2) from the fixed end. Although position X_5 could capture all resonance frequencies, it is not an option for the testing, since the accelerometer is closer to the tip of the sample and will represent higher amplitudes for modal mode 1. Taking a look into the values reported in Table 3.3-3, the damping coefficient difference captured is quite notable for the same probe with same accelerometer (in this case 4508-1 used) and test parameters, but different position, especially for mode 1.

Table 3.3-3: Damping coefficient for same probe but different accelerometer positions

Mode	X_2	X_5
1	0.29%	5.50%
2	1.02%	2.15%
3	0.42%	0.55%
4	0.21%	0.57%
5	0.60%	0.56%

With this study it can be advised to the reader to run a FEA from any sample or structure to be tested before placing the sensor in a random position. Also, as seen from the study previously mentioned, the experimental results strongly correlate with the analysis purely

done in ABAQUS software. For future testing's mathematical model analysis could be a tool to use, replacing the trial and error from physical experiment saving time.

To finalize and complement this study different probe lengths were model in ABAQUS to further parametrize an ideal length were to place the sensor in rectangular shape probes. The conclusion is to set the sensor at a 0.6*L distance from the fixed end. Where L represents the total length of the probe.

3.4. Damping Calculation

To obtain the damping coefficient as previously mentioned in past sections, a pseudo random excitation will be used to get the natural frequencies of each sample and then apply the half-power bandwidth method described early in Section 2. With this method the major drawback is the resolution of the data obtained. Since the experimental testing will consider the first five modal frequencies, the studied frequency range will be (0 - 3.2)kHz according to FEA results. The wide analysis may cause the data acquisition and processing of the response be inaccurate, especially for the first modal modes. For example, for sample (*S_G45_Si*) the first mode damping factor is about 17.69% with the half-power bandwidth method, as it can be seen on Figure 3.4-1. This is a very big value most probably not true for the material. For this reason, two proposed alternatives are presented in short, where different ways can reach into better results.

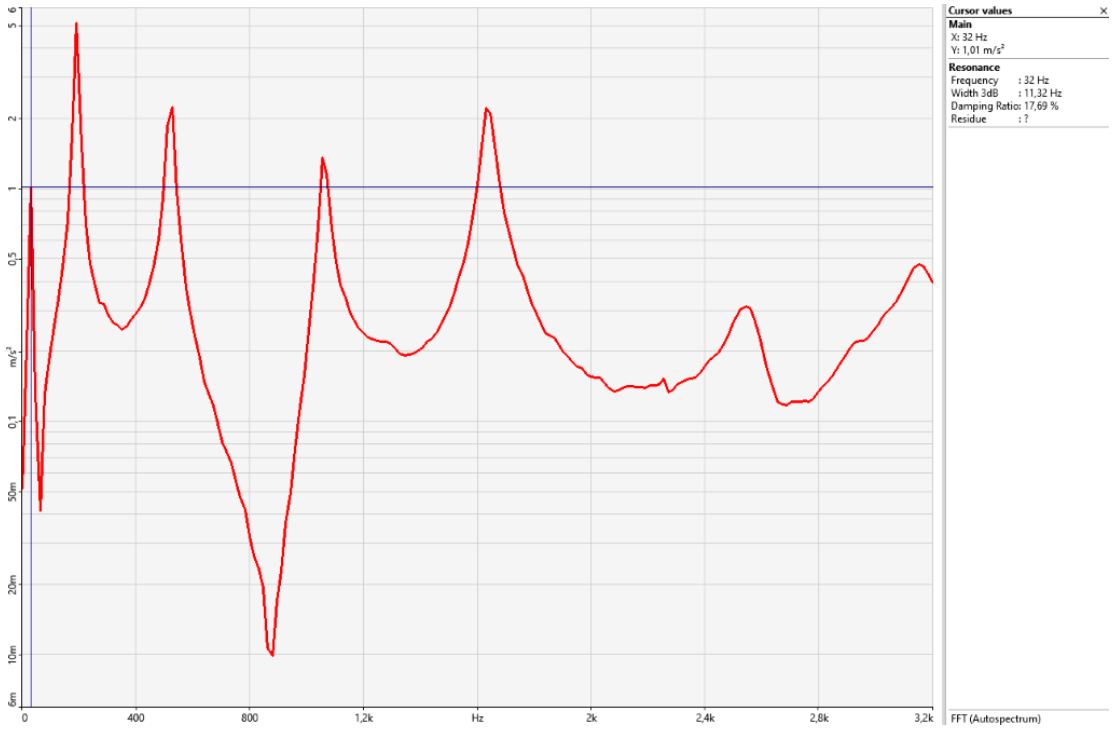


Figure 3.4-1: Sample (*S_G45_Si*) first mode damping factor

3.4.1. Zoom Analysis

The Zoom analysis consists on performing an emphasis on each of the modal modes of the sample. After finding the resonance peak in the wider test, the zoom analysis will focus on a limited bandwidth (50 Hz) centred on each of the natural frequencies. In this case a periodic random signal was chosen to minimize leakage error but also improve the signal quality acquisition. However, this study will take some time to get a result, since significant number of data have to be obtained to ensure an average value, hence a correct experiment [16]. An example of the sample (*S_G45_Si*) FRF can be seen in Figure 3.4-2. Note the accuracy and how much the value changed compared with the one presented in Figure 3.4-1. From 17.69% to 3.98% it is confirmed, the damping ratio is drastically affected by the method and signal bandwidth used.

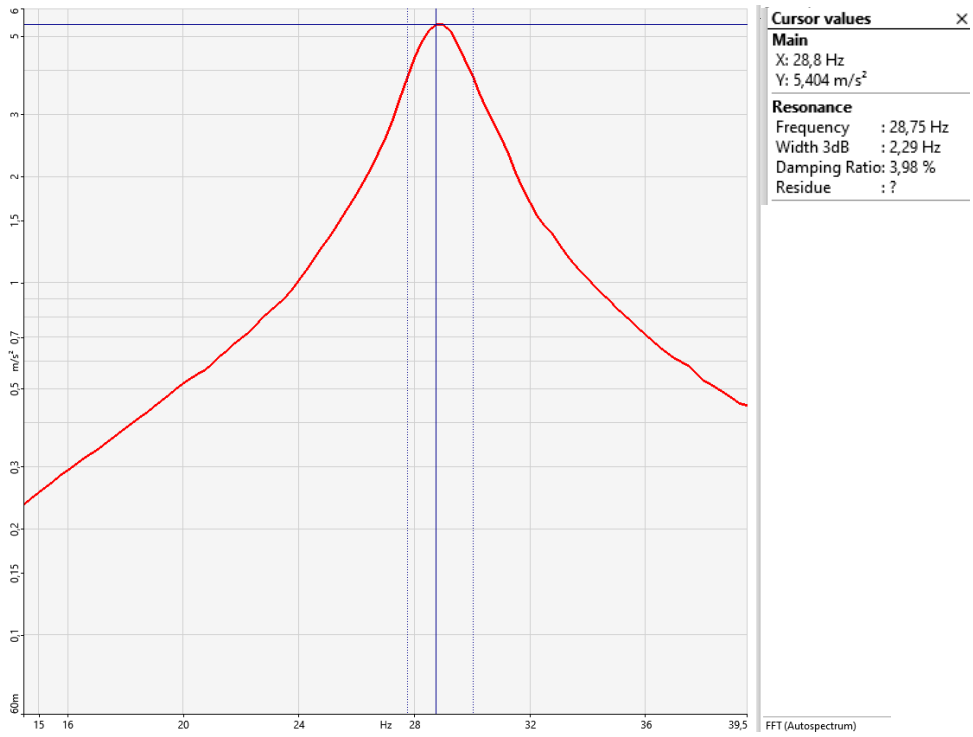


Figure 3.4-2: Zoom analysis, Sample (*S_G45_Si*) first mode damping factor

3.4.2. Reverberation Time

An alternative to the long and time-consuming Zoom method, the same B&K supplier propose a different way to obtain the damping coefficient when transient signal is used. For the case with shaker induced vibrations, the pseudo random excitation study can be used as an input signal, to further apply a weighting function that will get us the impulse response function (IRF). By analysing the time it takes the signal to attenuate after the resonance peak, term known as decay rate (σ), damping coefficient can be calculated with Eq. (3.4-1). Subsequently the decay rate is related to the time constant (τ) Eq. (3.4-2), which is the time the signal takes to lower 20loge = 8.7dB. This number comes from the reverberation time principle, when engineers look for how much time it takes for a signal to stabilize after excitation. Normally it is done with 60dB but in noisy environment or study, the T20 can be used. The main advantage of this method is that, the wideband analysis with pseudo random excitation can be used to get the different damping values from different modal modes. There is no necessity on

performing additional test on each natural frequency and the resolution of the result should not be a problem if the procedure is followed correctly [17].

$$\zeta_n = \frac{\sigma}{2\pi f_n} = \frac{1}{\tau 2\pi f_n} \tag{3.4-1}$$

$$\tau = \frac{1}{\sigma} \tag{3.4-2}$$

In the following Figure 3.4-3 a representation of the IRF for the sample (*S_G45_Si*) is shown. For this case the damping factor calculated is about 1.9%. The value is quite different from the one obtained for the Zoom method. In theory for the first mode, it is expected an over estimation of the damping coefficient for the first resonance mode, but for the rest of the modal modes more accurate values are obtained with the Reverberation time method [17].

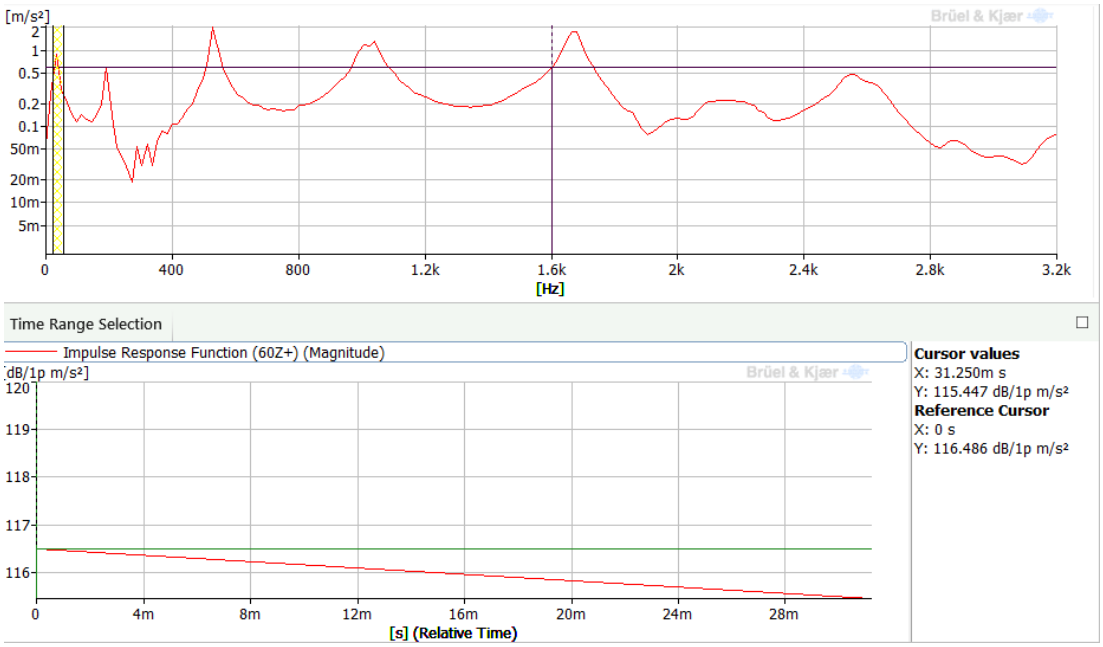


Figure 3.4-3: IRF for sample (*S_G45_Si*) for the first mode

THIS PAGE WAS INTENTIONALLY LEFT BLANK

4. RESULTS AND DISCUSSION

In this section results from the modal analysis are presented. This includes the natural frequencies, the damping factor and the modal shape for the probes. Additionally, a small statistical review on results from the same material but different samples is shown.

4.1. Natural Frequencies

To bear in mind the testing done to obtain the natural frequencies of the samples, a wide bandwidth of frequencies [0-3.2] kHz with a pseudo random excitation waveform was used. The experimental results obtained were easy to compute and strongly agree with the ones calculated by FEA. In Table 4.1-1 a comparison between both method results is shown for the first five modal modes. Additional in Figure 4.1-1 the FRF graph shown for the sample (*S_G45_Si*), where clearly it can be seen the peak resonance points of every natural frequency. For graphs regarding the rest of the samples refer to Appendix III.

Table 4.1-1: Natural frequencies for first five modal modes for each sample

Sample	Method	Mode				
		1	2	3	4	5
S_G00_Si	FEA	16	112	326	649	1077
	Exp.	20	148	432	864	1310
S_G00_Ak	FEA	16	112	326	649	1077
	Exp.	16	120	352	710	1073
S_G45_Si	FEA	26	169	483	955	1585
	Exp.	32	192	528	1060	1630
S_G45_Ak	FEA	26	169	483	955	1585
	Exp.	32	181	517	1063	1640
S_F00_Si	FEA	15	117	345	687	1134
	Exp.	20	108	320	656	1015

From the results obtained it is important to mention the FEA model does not consider the damping property of the material, therefore a slight difference is expected in the natural frequencies. Also, for this simulation the 4th FEA approach mentioned in Section 3.2.3 was used, the model with the added mass of the accelerometer to the whole assembly. Other

factors that were excluded from the experimental testing are the air and temperature damping. Although oscillations in the material were kept with small amplitude, there were no temperature sensors that could confirm the sample was at every moment from the test within the elastic region.

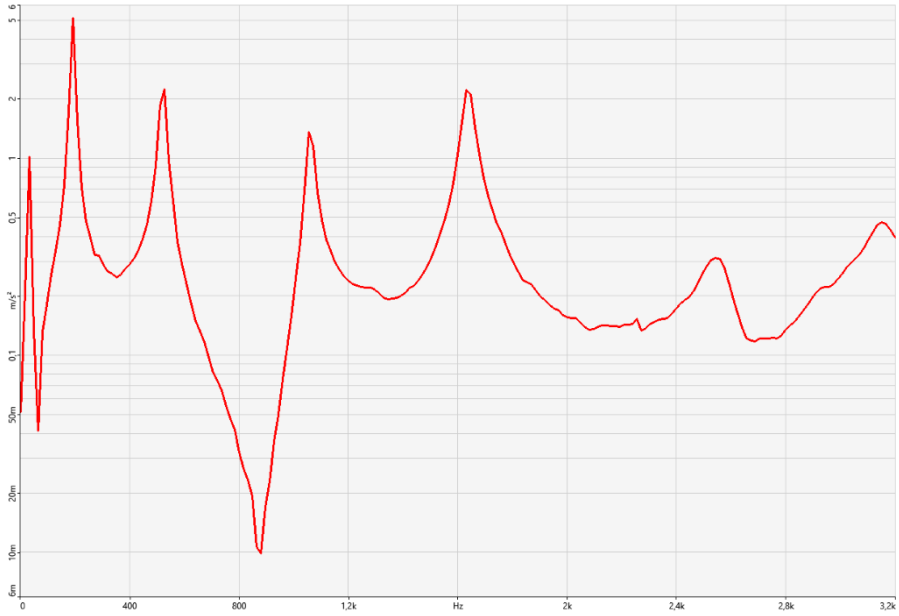


Figure 4.1-1: Frequency Response Function (FRF) of sample (*S_G45_Si*)

Another point to remark in this study is that for the low weight samples, [*S_G00_Si; S_G00_Ak; S_F00_Si*] two studies were conducted. One that had same parameters as the rest of materials and another one reducing the bandwidth to [0-1.6] kHz, to improve the resolution on the measurement, since FEA results showed the first five modes were expected below the 1.6kHz frequency. A comparison of both parameters study is presented in Table 4.1-2 for the (*S_G00_Si*) sample. Values are quite similar, but the main difference relies when obtaining the damping coefficient by the half-power method, especially for the first modal mode. It is clearly that for the wider bandwidth an overestimation of the damping factor could happen. Just looking how drastically the value reduced from 74% to 12%, it is sufficient justification to perform studies with reduced bandwidth for low weight samples. To keep track of the results presented so far, the numbers shown in Table 4.1-1 are the average of natural frequencies obtained with both methods for samples [*S_G00_Si; S_G00_Ak; S_F00_Si*], and for the heavier probes [*S_G45_Si; S_G45_Ak*] the only result with the wider bandwidth.

Table 4.1-2: Comparison on different bandwidth studies for sample (*S_G00_Si*)

Bandwidth	Natural frequencies					Damping 1st mode
	1	2	3	4	5	
[0-3.2]	16	144	432	864	1310	74.58 %
[0-1.6]	24	152	432	864	1310	12.39 %

4.2. Damping Coefficient

As mentioned before in Section 3 different approaches were conducted to obtain the damping coefficient. The studies performed were on a single sample for each different composite material. For the reverberation time method results can be seen in Table 4.2-1. This is a fast and simple way to obtain the results, however values computed are done manually and discrepancy from each modal mode is high.

Table 4.2-1: Damping coefficient [ζ] with reverberation time method

Sample	Frequency modes				
	1	2	3	4	5
S_G00_Si	2.98%	0.86%	0.11%	0.10%	0.78%
S_G00_Ak	5.36%	1.88%	1.80%	0.51%	2.04%
S_G45_Si	1.90%	2.32%	0.81%	0.84%	0.52%
S_G45_Ak	0.17%	1.57%	0.15%	0.18%	0.45%
S_F00_Si	0.08%	0.13%	2.56%	0.64%	0.12%

Different approach with the half-power bandwidth is presented in Table 4.2-2. Here all the results are obtained directly from the software. No calculations are required and the single pseudo random excitation used for the wide frequency band is used. From this method the results are most probably overestimated for the first two modal modes. This is the reason to adopt the Zoom Analysis presented In Section 3.4 and therefore the results obtained in Table 4.2-3 are a combination of the zoom analysis and the values obtained directly from software for the third, fourth and fifth modal modes. To remember the reader, the zoom analysis requires an additional test excitation and new measurement recorded only dedicated for the frequency of interest. Values obtained are similar and around the same order of magnitude for the second to fifth modal modes. Only for the first mode, the damping coefficient still shows a high value in comparison with the next modes.

Table 4.2-2: Damping coefficient [ζ] with half-power bandwidth method

Sample	Frequency modes				
	1	2	3	4	5
S_G00_Si	12.39%	3.64%	0.82%	0.60%	1.12%
S_G00_Ak	18.34%	3.58%	1.28%	0.59%	0.56%
S_G45_Si	17.69%	3.58%	2.75%	1.51%	1.35%
S_G45_Ak	18.76%	4.67%	1.57%	1.76%	1.59%
S_F00_Si	13.78%	4.06%	1.15%	1.85%	0.90%

Table 4.2-3: Damping coefficient [ζ] with mixed methods

Sample	Frequency modes				
	1	2	3	4	5
S_G00_Si	4.31%	0.62%	0.82%	0.60%	1.12%
S_G00_Ak	7.68%	1.01%	1.28%	0.59%	0.56%
S_G45_Si	3.77%	0.95%	2.75%	1.51%	1.35%
S_G45_Ak	5.11%	1.77%	1.57%	1.76%	1.59%
S_F00_Si	3.41%	2.01%	1.15%	1.85%	0.90%

Important to recall, that for Sample (*S_F00_Si*) the total weight of the probe is 3.2g. This represents a problem when obtaining the natural frequencies and damping coefficient for this material. Since the mass of the sensor is around 18.7% of the total sample, the influence it has on the whole system is considerable high (according to B&K [8]), and so the measurements recorded could be substantially different from the real values. For this reason, no further studies will be done to the flax fibre material. To overcome this problem the simplest solution would be; to manufacture probe samples with larger thickness to consequently have more mass of the composite and so the sensor does not influence on the experimental testing. Other solution could be also to use contactless measurement devices, capable of getting a reading without affecting the mass of the system.

Although the main objective of this dissertation is to define a procedure for experimental testing, the values obtained in this project follow the references values found by other authors in the literature review presented in section 2. The results obtained in Table 4.2-3 are presented in Figure 4.2-1 for better comparison. Fibre orientation plays indeed a big influence in damping factor. The samples S_G45_Si and S_G45_Ak with a 45^{o} fibre orientation, colour graphs light blue and yellow, have almost the double damping coefficient as the same material but with unidirectional fibre orientation. Comparing the use on thermoplastics against

thermosets, the results are quite similar, not a big difference on the damping coefficient computed from the half-power bandwidth method. Looking at the glass 0º fibre orientation materials, colour graphs blue and red, both materials remain within the same range of values. Probably for the first two modal modes could be a notable difference between both matrices. Nonetheless obtaining experimental data for low frequency range is quite difficult and more prompt to error and noise in the data recorded. Finally, even considering the mass influence of the accelerometer to the system, the flax fibre (green graph) showed values of damping higher than the ones found on glass fibre materials with same 0° direction. This value should be reconfirmed with proper experiment configuration, nonetheless it confirms that natural fibres tend to have better damping response as synthetic fibres [14].

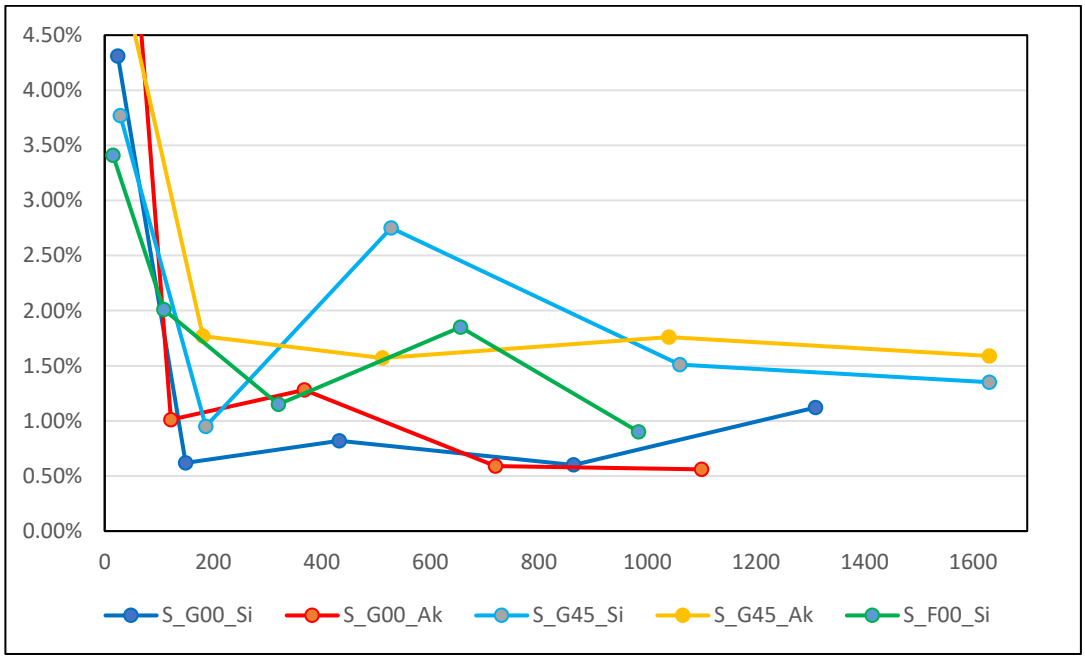


Figure 4.2-1: Data from the Table 4.2-3

Nevertheless, the experimental testing done was only with one sample of each composite, and so the results of every material lack on statistical data to be true. It can be seen for example, in the light blue graph (*S_G45_Si*) the data has strange peaks at the second and third mode of vibration. For having a real and more reliable value more samples of the same production batch of the composite should be tested, and further obtain the reference value with statistical analysis.

4.2.1. Statistical analysis

Fortunately, three samples of the same material (*S_G45_Ak*) were available for testing. Although it is not sufficient probes to have a statistical sample, the three probes were similar in geometry and properties. There is no data recorded from the moisture content on each of the sample, but it will be considered that all of them come from the same batch and with the same quality manufacturing process. In Table 4.2-4 the results are shown for natural frequencies and damping coefficient using half-power bandwidth method for the three samples. Also, the coefficient of variation (CoV) and mean is presented for each category of interest. The Table 4.2-5 presents the same information but using the reverberation time method for the same samples.

Table 4.2-4: Nat. freq. and damping coeff. for (S_G45_Ak) samples with half-power bandwidth method

Mode	Category	S1	S2	S3	Mean	CoV
1st	Nat. Freq. [Hz]	32	32	32	32	0.00%
	Damp. coeff. [%]	5.69%	5.11%	5.12%	5.31%	6.26%
2nd	Nat. Freq. [Hz]	176	176	192	181	5.09%
	Damp. coeff. [%]	1.74%	1.77%	1.85%	1.79%	3.18%
3rd	Nat. Freq. [Hz]	512	512	528	517	1.79%
	Damp. coeff. [%]	1.56%	1.57%	3.25%	2.13%	45.75%
4th	Nat. Freq. [Hz]	1060	1040	1090	1063	2.37%
	Damp. coeff. [%]	1.30%	1.76%	1.70%	1.59%	15.76%
5th	Nat. Freq. [Hz]	1630	1630	1660	1640	1.06%
	Damp. coeff. [%]	1.72%	1.59%	2.05%	1.79%	13.27%

With the results obtained some conclusions from the statistical analysis can be computed. The method used has a strong influence on the final value computed. For the reverberation time method, the values are very different one from each other, among the samples. The high CoV indicates probably a wrong computation or an inaccurate method to use when comparing even the same material. For the values computed using the half-power bandwidth method a strong correlation showed by the low variation among the three samples. Just for the third mode it can be seen a +30% CoV, which value is questionable, since the third sample showed a value which was higher than twice that value for the first and second probes. With more samples recorded the third value could be statistically excluded and so the average computed may have lower CoV. After this point, it is advised to the reader to follow the mixed method,

performing a zoom analysis for the first two modal modes and obtaining the values directly from the software without manual computation.

For most applications a constant value of damping coefficient (independent of the frequency) is generally considered. For this purpose, an average of the values from the second to fifth modal mode is calculated, leaving the data from the first resonance peak outside the characterization, because of the reasons exposed above. For these three samples of glass fibre with Akelite matrix, the general damping coefficient is around 1.8% with a coefficient of variation around 12.3% among the data. This means, the value is representative for the four different modes and different samples. For other samples this calculation could also be used to obtain the general characterization of the material as shown in Table 4.2-6.

Table 4.2-5: Nat. freq. and damping coeff. for (S_G45_Ak) samples with reverberation time method

Mode	Category	S1	S2	S3	Mean	CoV
1st	Nat. Freq. [Hz]	32	32	32	32	0.00%
	Damp. coeff. [%]	5.25%	0.17%	0.12%	1.85%	159.83%
2nd	Nat. Freq. [Hz]	176	176	192	181	5.09%
	Damp. coeff. [%]	2.19%	1.57%	0.87%	1.55%	42.75%
3rd	Nat. Freq. [Hz]	512	512	528	517	1.79%
	Damp. coeff. [%]	2.60%	0.15%	0.41%	1.06%	127.42%
4th	Nat. Freq. [Hz]	1060	1040	1090	1063	2.37%
	Damp. coeff. [%]	0.18%	0.18%	0.35%	0.24%	43.18%
5th	Nat. Freq. [Hz]	1630	1630	1660	1640	1.06%
	Damp. coeff. [%]	0.87%	0.45%	0.20%	0.51%	66.76%

Table 4.2-6: Mean damping coefficient [ζ] excluding first mode

Sample	Damping coefficient	CoV
S_G00_Si	0.79%	30.56%
S_G00_Ak	0.86%	40.38%
S_G45_Si	1.64%	47.35%
S_G45_Ak	1.82%	12.30%
S_F00_Si	1.48%	36.30%

4.3. Modal shapes

To obtain the modal shapes multiple tests were performed moving the sensor through different positions. The test configuration remains the same as the one used to obtain natural frequencies, just the sensor was moved from position X_1 to X_5. This means from 100mm to 180mm from the fixed end respectively. After then in the B&K Connect software, the recorded data was associated to a virtual model of the probe. Setting the coordinate of the sensor to a node position on the model.

After combining the five recorded data for the sample (S1_G45_Ak) the software delivered images of the model like the one in Figure 4.3-1. Every peak of the triangles represents the accelerometer position and the maximum displacement it had during the excitation at the named mode. Comparing the displacement recorded by the test with the FE simulation it can be seen a strong correlation on the displacement expected with the real one measured from tests. In Appendix IV more images about the different mode displacements can be founded.

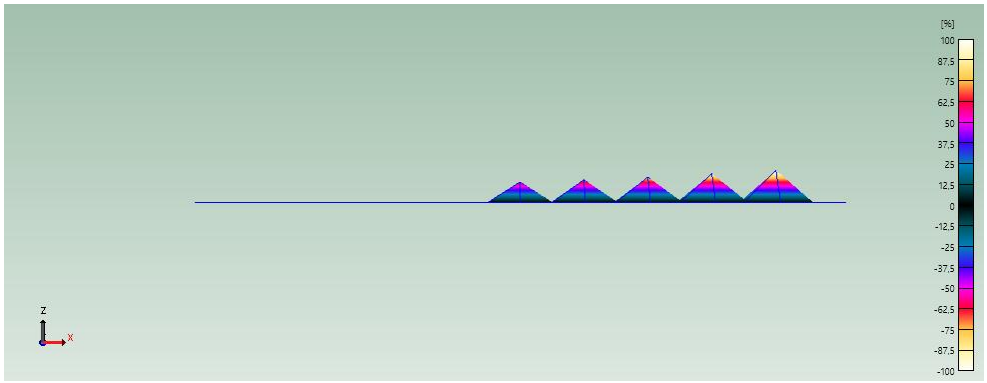


Figure 4.3-1: First modal shape obtained by experimental testing

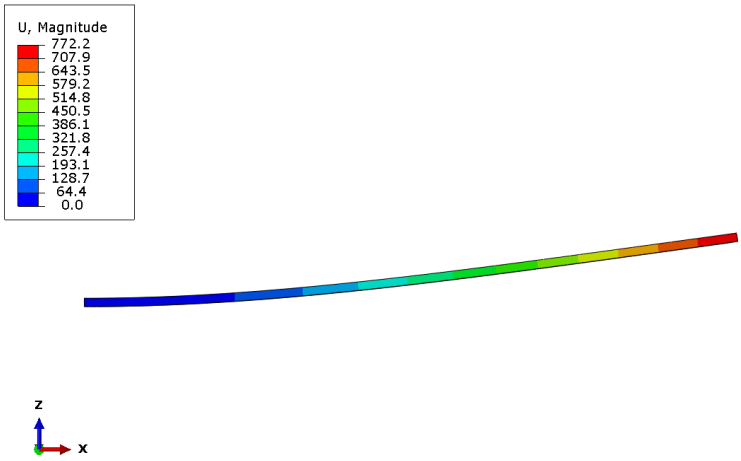


Figure 4.3-2: First modal shape obtained by FE model

THIS PAGE WAS INTENTIONALLY LEFT BLANK

5. CONCLUSION

This dissertation presented a detailed procedure on how to perform dynamic characterization for composite materials. Experimental testing procedures currently lack on certified norms and regulations to follow, nonetheless polymer standards were followed whenever possible. The Literature Review together with the Methodology section presented information useful to the reader, to understand how damping coefficient can be obtained. In Section 4 experimental results are presented, together with some discussion on the data collected. Below the main summary and conclusions from the project, as well as comments and further steps or recommendations for research improvement are presented.

5.1. Main Conclusions

The procedure followed in this project showed a good methodology supported by finite element analysis. The modelling of the material samples together with the mechanical attachment design validated that the metallic part would not interfere on vibrations exerted to the samples, delivering a starting position from where to expect the resonance frequencies, and therefore a useful parameter to consider in the experimental excitation profile.

For the Input signal Pseudo Random excitation is preferred, because of the leakage error prevention, as well as a fast computation on averages getting the experimental values. Half-power bandwidth method was used to obtain damping coefficient. For better signal acquisition at lower frequencies, Periodic Random signal would be used, as it was done for the Zoom analysis in the first and second mode, considering the computation time will increase for testing.

Sensors and instruments used to record data have to be carefully chosen and strategically positioned within the system to analyse. Section 3.3.2 showed a detailed trial performed on different sensor positions within the material sample length. Information obtained from ABAQUS simulation was useful to find an optimal distance from the fixed end. In the case of rectangular shape samples with one end fixed, like a cantilever beam experimental configuration, it is advised to place the sensor at 0.6 the length of the probe from the base

(fixed end). For other projects, parts, shapes and experiments it is advised to the reader to perform this type of FE models to find the appropriate position.

From the data obtained for damping coefficient it clearly needed a larger number of samples to conclude on a specific value of statistical significance. The coefficient of variation on the three samples showed that some modes could vary and therefore new tests and additional probes are needed to conclude on a representative value. Also, it was found for all the materials that damping coefficient in the first modal mode is significantly higher than the rest of the modes. For this reason, an average value from second resonance mode through five can be calculated and used for material characterization.

5.2. Further developments

The first mode of resonance seems to appear at a low level of frequency, this creates challenging scenarios to collect data from the samples. For this reason, it is recommended to produce heavier, hence stiffer, material samples. With this improvement light damped systems are avoided and so the noise in experimental data recorded have less influence and inherence on the result computed. With thicker probes the sample mass will increase, in this way the lightweight composites are not affected by the instrumentation, as it was for the flax fibre sample.

It is advised also to revise the temperature range at which sensors can work properly and try to reproduce the same experiment but with temperature variable control. An Interesting area of research for materials that will be used in demanding environments, since the viscoelasticity of the matrix is more prompt to change when temperature fluctuate.

6. REFERENCES

[1] A. Treviso, B. Van Genechten, D. Mundo and M. Tournour, "Damping in composite materials: Properties and models," *Composites Part B: Engineering,* vol. 78, pp. 144-152, 2015.

[2] P. D. Mane, A. A. Yadav, A. M. Pol and V. A. Kumbhar, "COMPARATIVE ANALYSIS OF NATURAL FREQUENCY FOR CANTILEVER BEAM THROUGH ANALYTICAL AND SOFTWARE APPROACH," *International Research Journal of Engineering and Technology (IRJET),* vol. 05, no. 02, p. 656–671, February 2018.

[3] S. K. Bhudolia, P. Perrotey and S. C. Joshi, "Enhanced vibration damping and dynamic mechanical characteristics of," *Composite Structures,* vol. 179, pp. 502-513, 2017.

[4] S. H. Dashatan, M. Sit, Z. Zhang, E. Grossmann, J. Millot, Y. Huang and . H. N. Dhakal, "Enhanced vibration damping and viscoelastic properties of flax/epoxy composites and their carbon fibre hybrid laminates," *Composites Part A: Applied Science and Manufacturing,* vol. 175, p. 107819, December 2023.

[5] R. D. Adams and D. G. C. Bacon, "Measurement of the flexural damping capacity and dynamic Young's modulus of metals and," *Journal of Physics D: Applied Physics,* vol. 6, pp. 27-41, 1973.

[6] S. A. Suarez, R. F. Gibson and L. R. Deobald, "Random and Impulse Techniques for Measurement of Damping in Composite Materials," *Experimental Techniques,* vol. 8, pp. 19-24, 1984.

[7] J. Vanwalleghem, I. De Baere, M. Loccufier and W. Van Paepegem, "External damping losses in measuring the vibration damping properties in lightly damped specimens using transient time-domain methods," *Journal of Sound and Vibration,* vol. 333, no. 6, p. 1596–1611, March 2014.

[8] Døssing, Ole; Brüel & Kjær, "STRUCTURAL TESTING Part I: Mechanical Mobility Measurements," Brüel & Kjær, Naerum, Denmark, 1988.

[9] P. Avitabile, Modal Testing: A Practitioner's Guide, Hoboken, NJ: John Wiley & Sons Ltd, 2018.

[10] . J. -M. Berthelot and Y. Sefrani, "Damping analysis of unidirectional glass and Kevlar Fibre Composites," *Composites Science and Technology,* vol. 64, no. 9, p. 1261–1278, July 2004.

[11] M. Kayaaslan, T. Coskun, O. S. Sahin, U. M. Unlu and F. Kadioglu, "Mechanical and dynamic responses of unidirectional/woven carbon fiber reinforced thermoset and thermoplastic composites after low velocity impact," *Polymers and Polymer Composites,* vol. 30, no. 1, pp. 1-11, January 2022.

[12] R. Chandra, S. P. Singh and K. Gupta, "Damping studies in fiber-reinforced composites – a review," *Composite Structures,* vol. 46, no. 1, pp. 41-51, September 1999.

[13] J. M. Kenny and M. Marchetti, "Elasto-plastic behavior of thermoplastic composite laminates under cyclic loading," *Composite Structures,* vol. 32, no. 1-4, pp. 375-382, 1995.

[14] F. Duc, P. E. Bourban, C. J. G. Plummer and J. -A. E. Månson, "Damping of thermoset and thermoplastic flax fibre composites," *Composites Part A: Applied Science and Manufacturing,* vol. 64, p. 115–123, September 2014.

[15] F. Orban, "Damping of materials and members in structures," *Journal of Physics: Conference Series,* vol. 268, no. 012022, 2011.

[16] A. W. Phillips and R. J. Allemang, "An overview of MIMO-FRF excitation/averaging/processing techniques," *Journal of Sound and Vibration,* vol. 262, no. 3, p. 651–675, May 2003.

[17] S. Gade and H. Herlufsen, "Digital Filter Techniques vs. FFT Techniques for Damping Measurements (Damping Part I)," Brüel & Kjær A/S, Nærum, Denmark, 1994.

APPENDIX I: MECHANICAL ATTACHMENT

Dimensions and specifications of the mechanical attachment designed are presented.

Figure A.I - 1: Technical Drawing of mechanical attachment

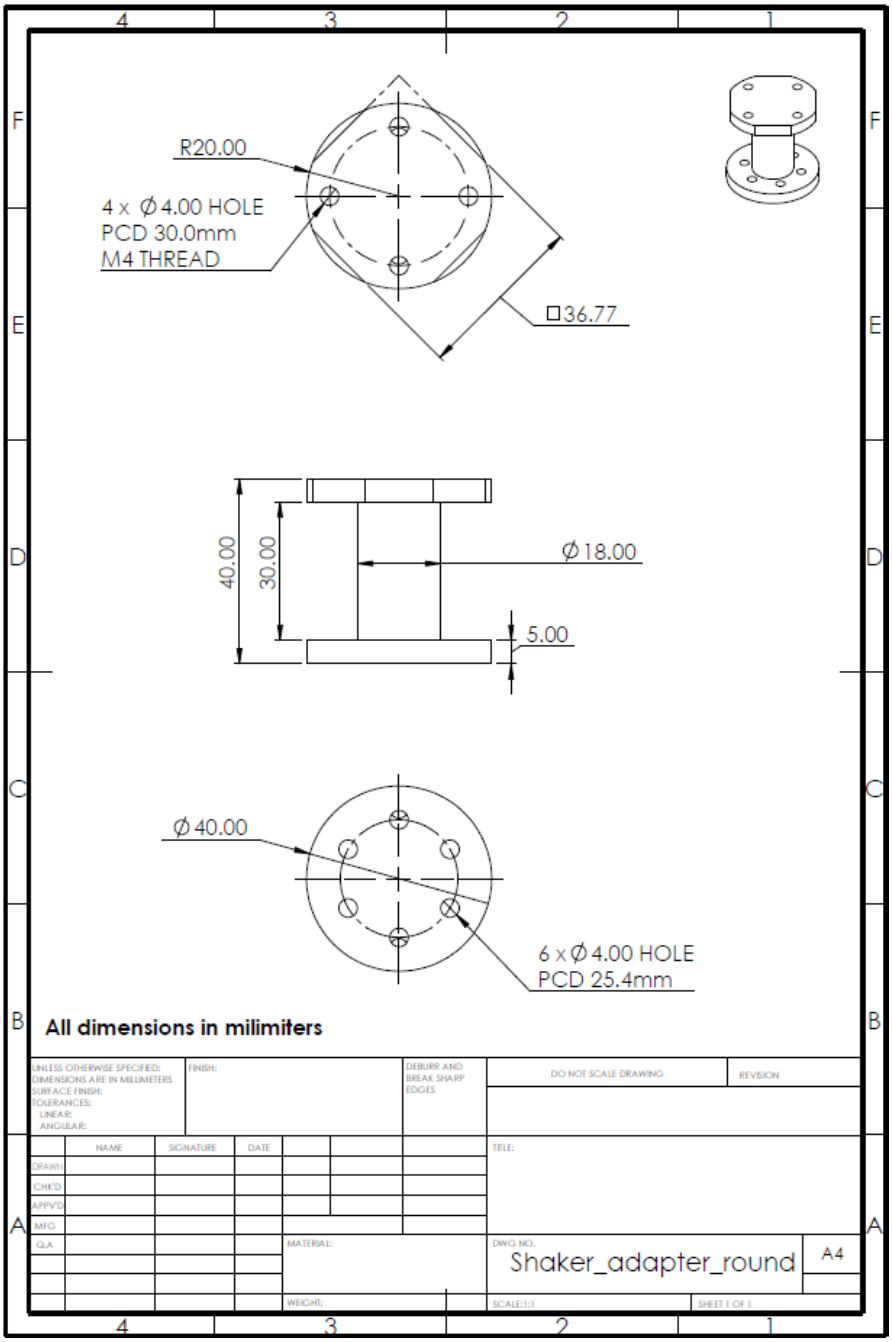
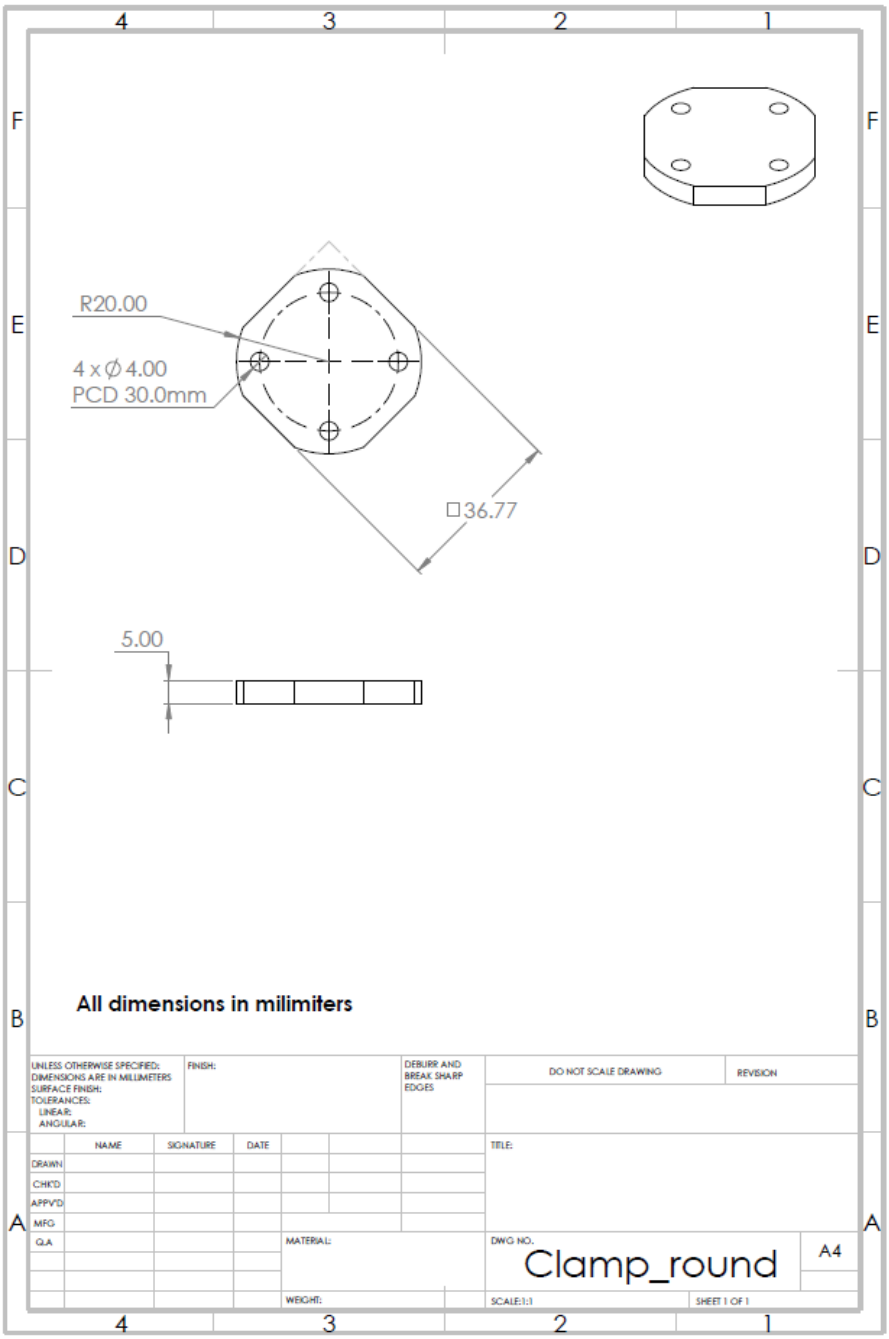


Figure A.I - 2:Technical Drawing of clamp attachment



APPENDIX II: FINITE ELEMENT ANALYSIS

Natural frequencies obtained by finite element methods for sample S_G45_Si. Each natural frequency is represented by the modal shape. The first 5 images show vibration modes for the probe alone. The following images represent same analysis but adding the mechanical attachment to the model. The objective is to compare shape and natural frequencies found.

Figure A.II - 1: Probe *S_G45_Si* first vibration mode (28 Hz)

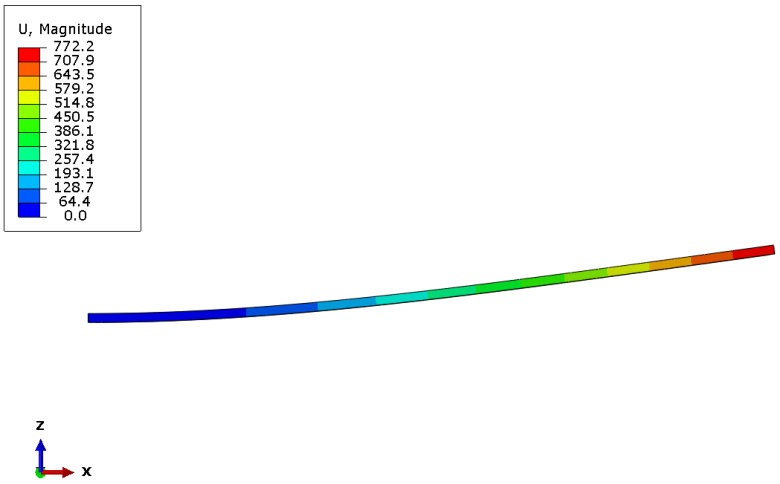


Figure A.II - 2: Probe *S_G45_Si* second vibration mode (173 Hz)

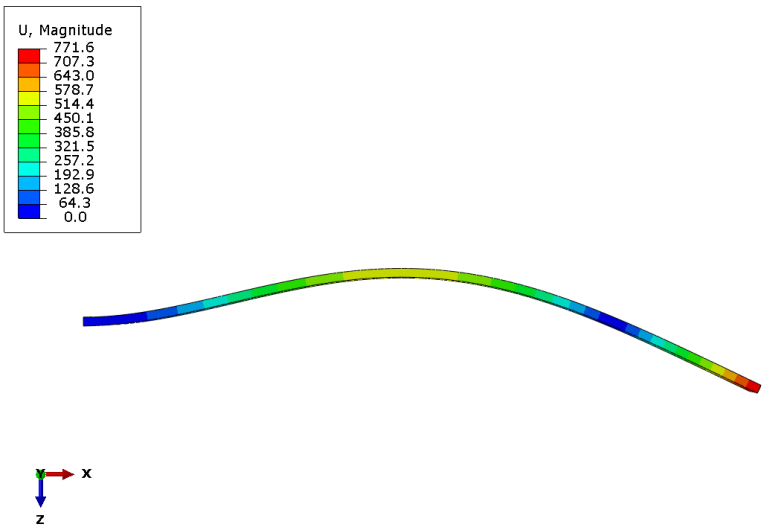


Figure A.II - 3: Probe *S_G45_Si* third vibration mode (485 Hz)

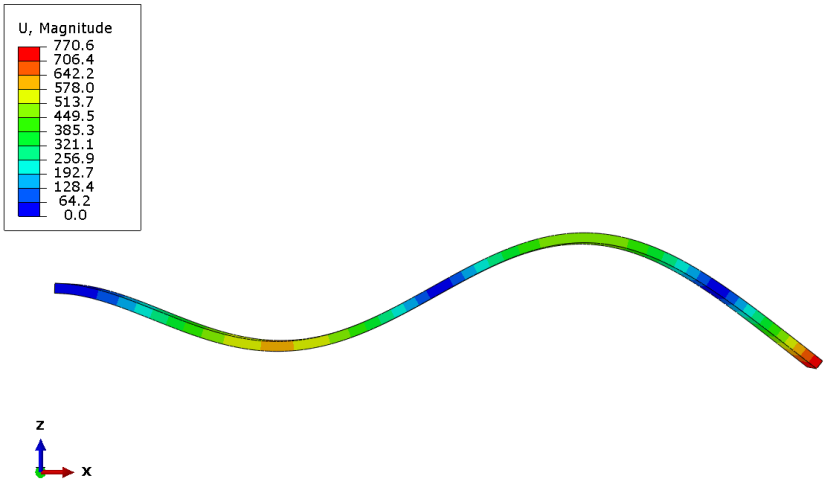


Figure A.II - 4: Probe *S_G45_Si* fourth vibration mode (947 Hz)

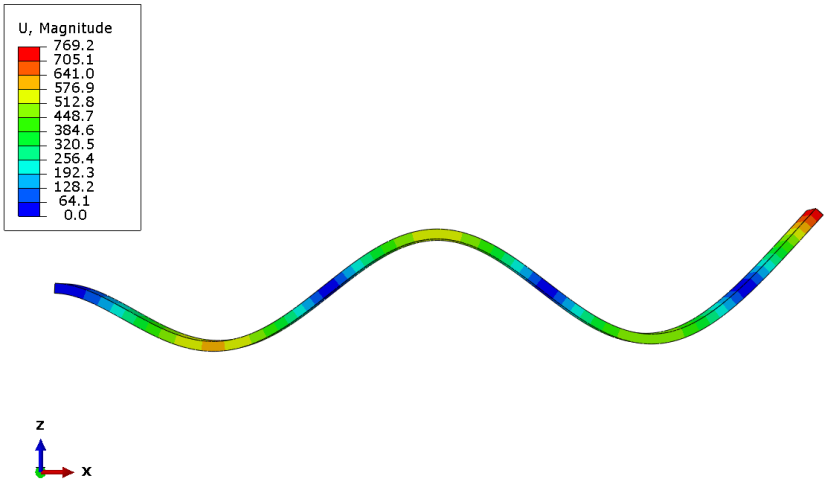


Figure A.II - 5: Probe *S_G45_Si* fifth vibration mode (1560 Hz)

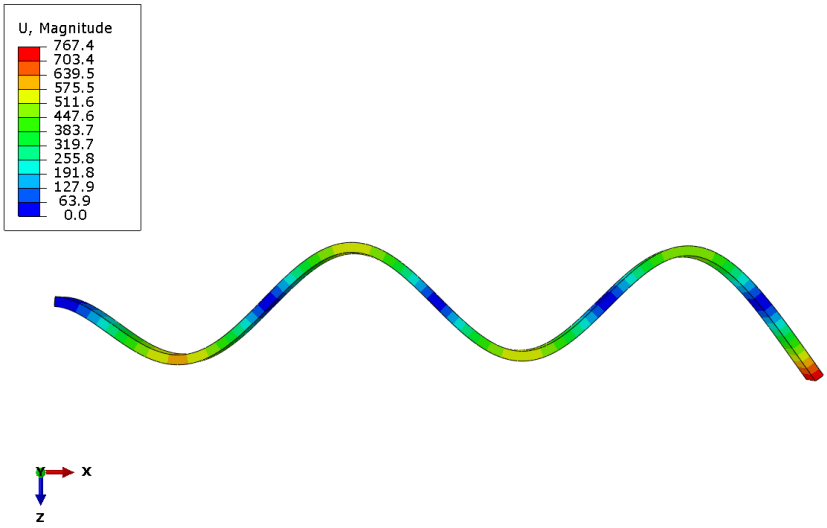


Figure A.II - 6: Assembly *S_G45_Si* first vibration mode (28 Hz)

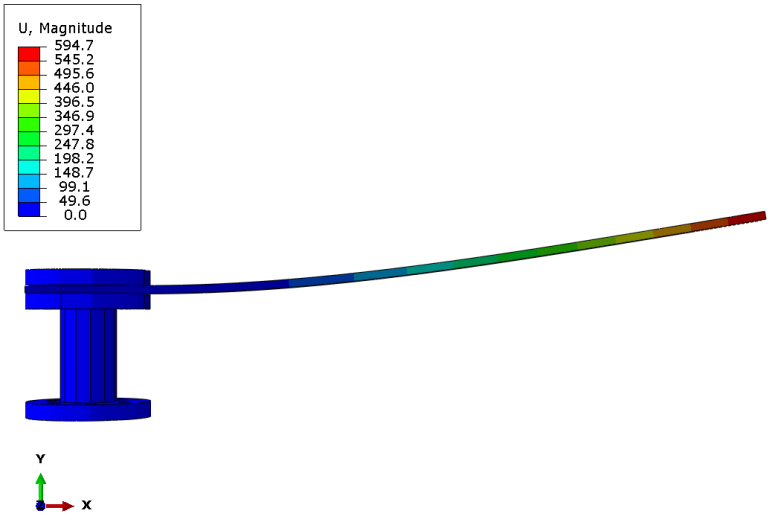


Figure A.II - 7: Assembly S_G45_Si second vibration mode (176 Hz)

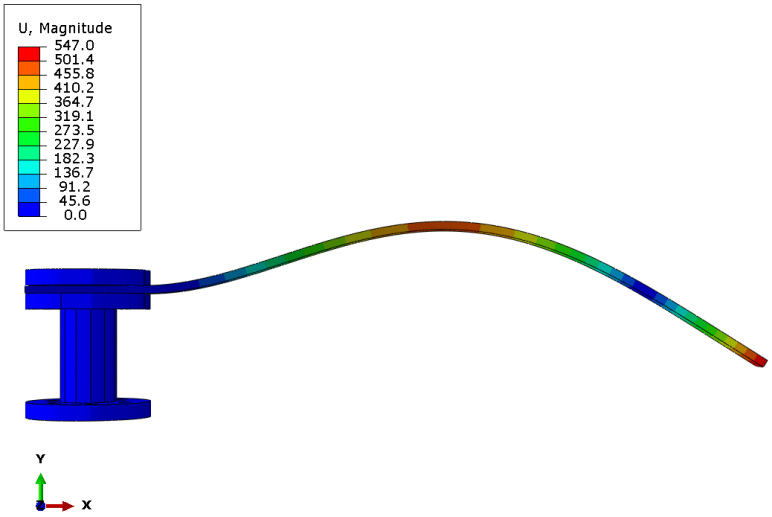


Figure A.II - 8: Assembly *S_G45_Si* third vibration mode (494 Hz)

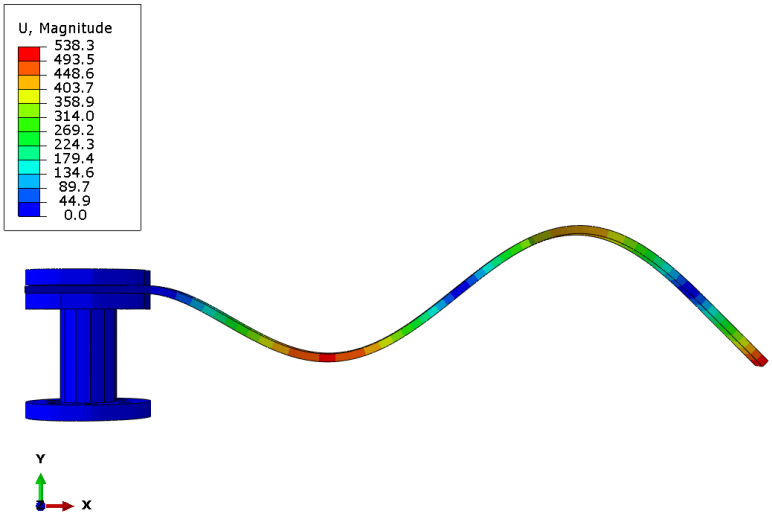


Figure A.II - 9: Assembly *S_G45_Si* fourth vibration mode (969 Hz)

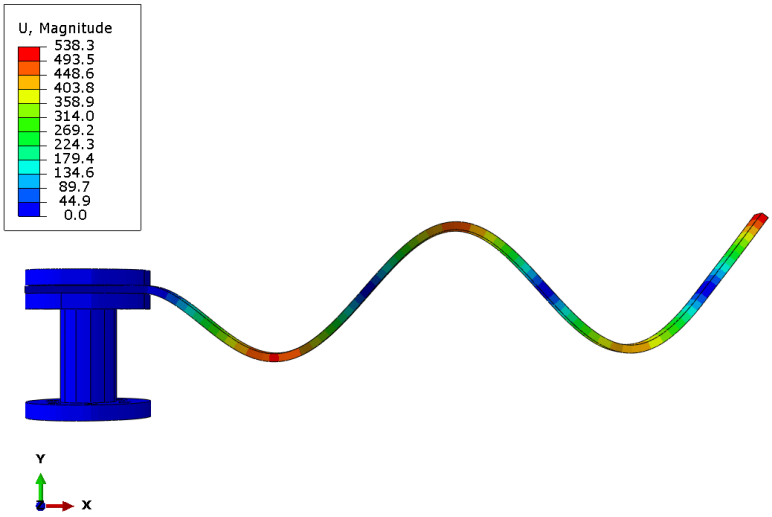
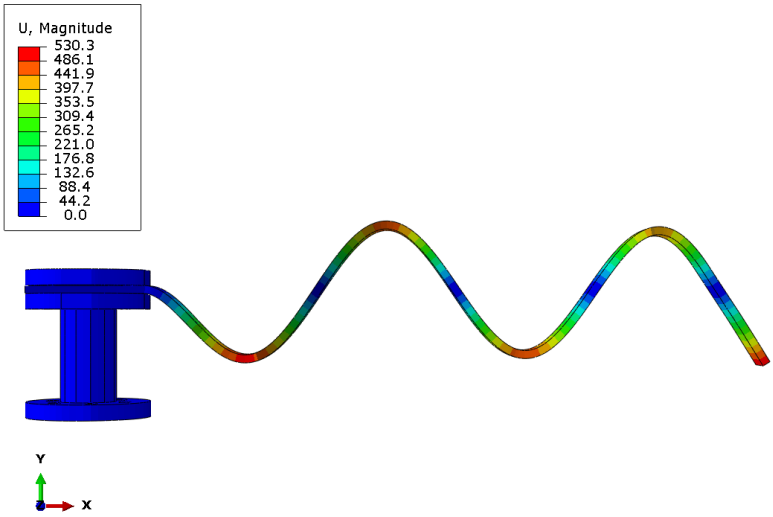


Figure A.II - 10: Assembly *S_G45_Si* fifth vibration mode (1608 Hz)



Next, it will be presented images regarding the finite element model to help the reader understand in further detail parameters used.

For the mesh, shell 4-nodes square (S4R) of 1mm length were used in the material probe. After running default mesh size and parametric one, same results were obtained. It was preferred to have 1mm length square mesh, to easily locate any coordinate, therefore the distance from the fixed end at any point. See Figure A.II - 11.

For the other mechanical components 10-node quadratic tetrahedral (C3D10) automatic size mesh was implemented since analysis in that area is not the concern. See Figure A.II - 12 and Figure A.II - 13.

For the glass fibres + sicomin characteristic values are presented in Table 3.2-1. For thermoplastic materials (Akelite) same properties were used. For the sample using flax fibre, characteristic values are shown in Figure A.II - 14.

Figure A.II - 11: Mesh of the probe, zoom in picture to clearly see the squares (avg. aspect ratio = 1.0)

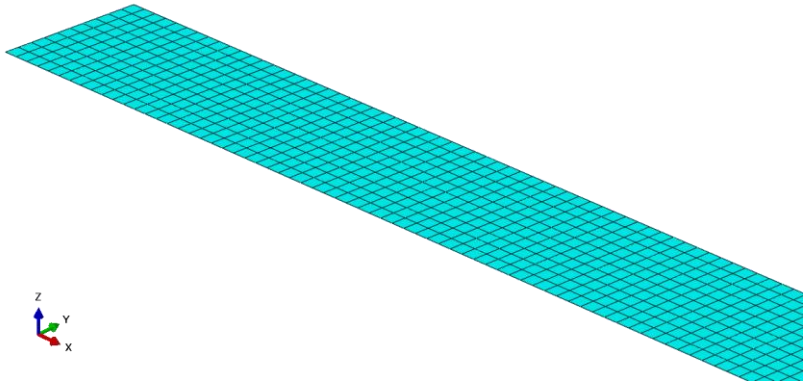


Figure A.II - 12: Mesh of mechanical attachment (avg. aspect ratio = 1.8)

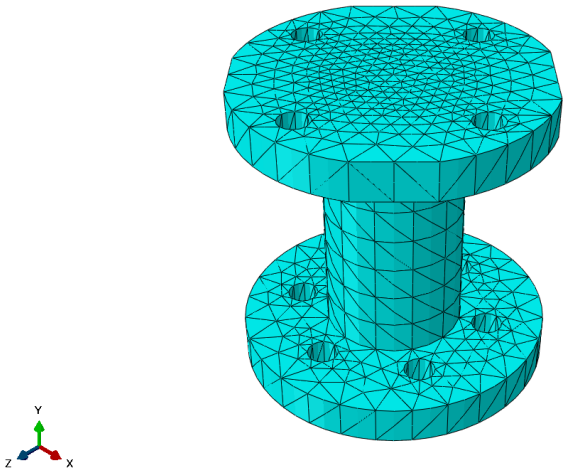


Figure A.II - 13: Mesh of clamp attachment (avg. aspect ratio = 1.6)

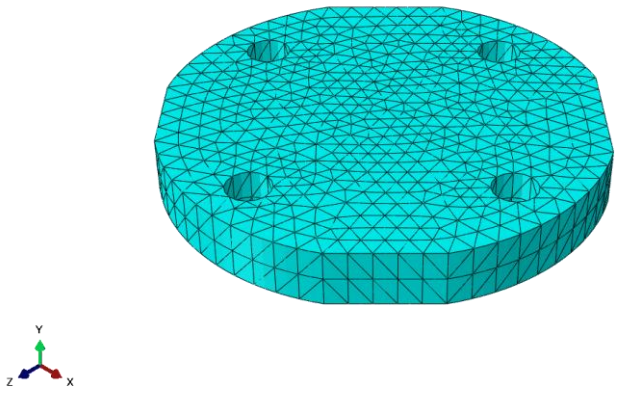
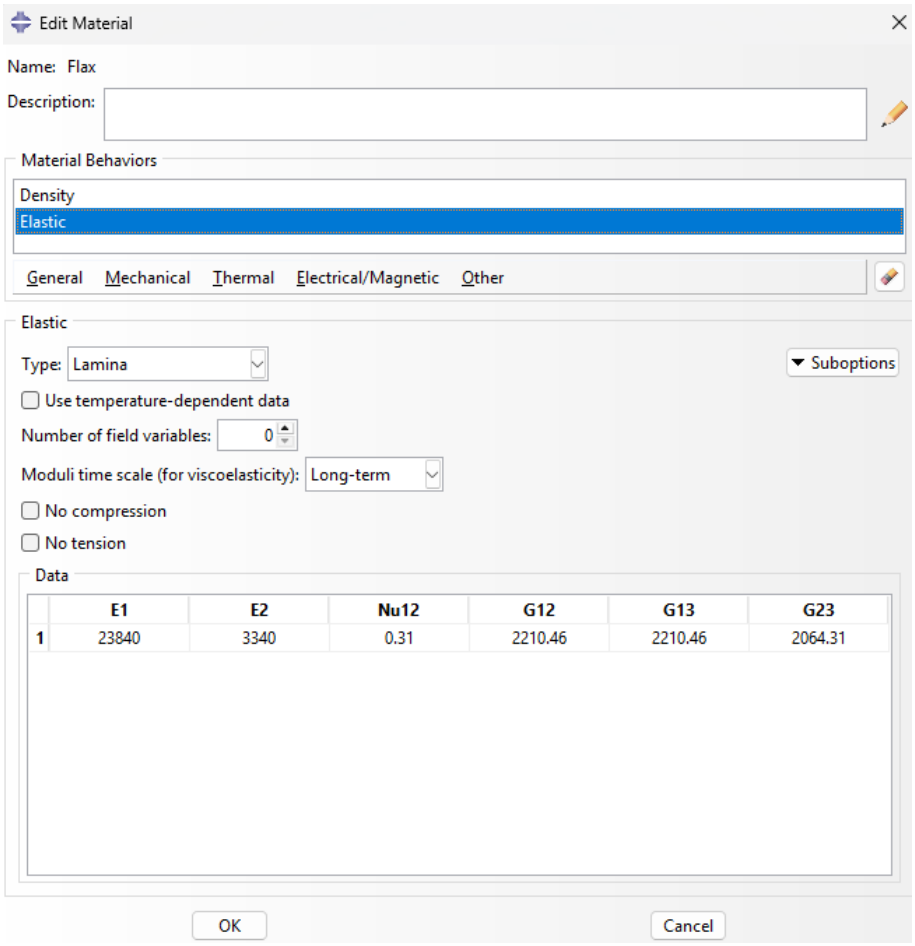


Figure A.II - 14: Flax characteristic values used in ABAQUS



Finally, the boundary conditions and interactions used in the model are shown in Figure A.II - 15 and Figure A.II - 16. All degrees of freedom (DOF) were fixed for the base of the mechanical attachment (ENCASTRE). For the upper clamp kinematic coupling constrained in all DOF, to simulate the bolts fixing both metallic parts. For the probe sample, the transverse axis had applied boundary conditions fixing the movement in transverse direction (Z axis in global coordinates) and the rotation around the other two axes. To simulate the contact between the probe and the mechanical attachment all DOF (ENCASTRE) condition was applied on the surface region adjacent between the material sample and the metallic attachment. At last, mass inertia was added to the assembly and coupled (kinematic, full constrained) to the surface of the probe to simulate the accelerometer mass in the model.

Figure A.II - 15: Boundary conditions in assembly model

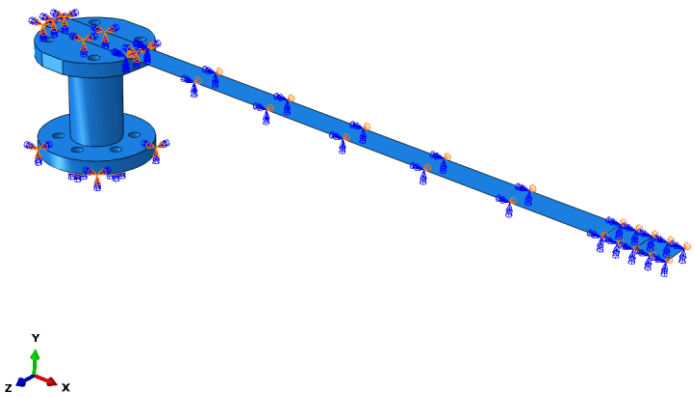
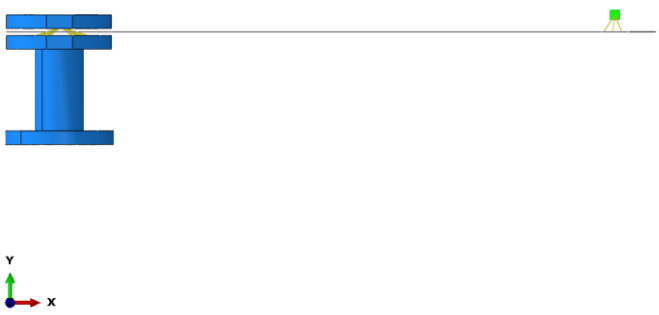


Figure A.II - 16: Interactions in assembly model



APPENDIX III: SAMPLES FRF

In this section the frequency response function (FRF) for the different samples is presented

Figure A.III - 1: Frequency Response Function for S_G00_Si

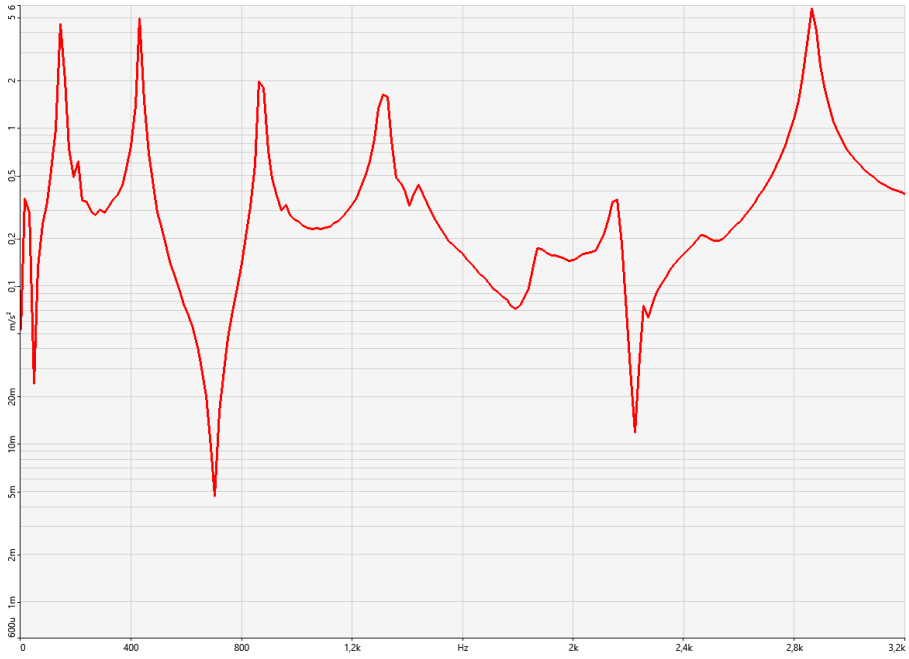


Figure A.III - 2: Frequency Response Function for S_G00_Ak

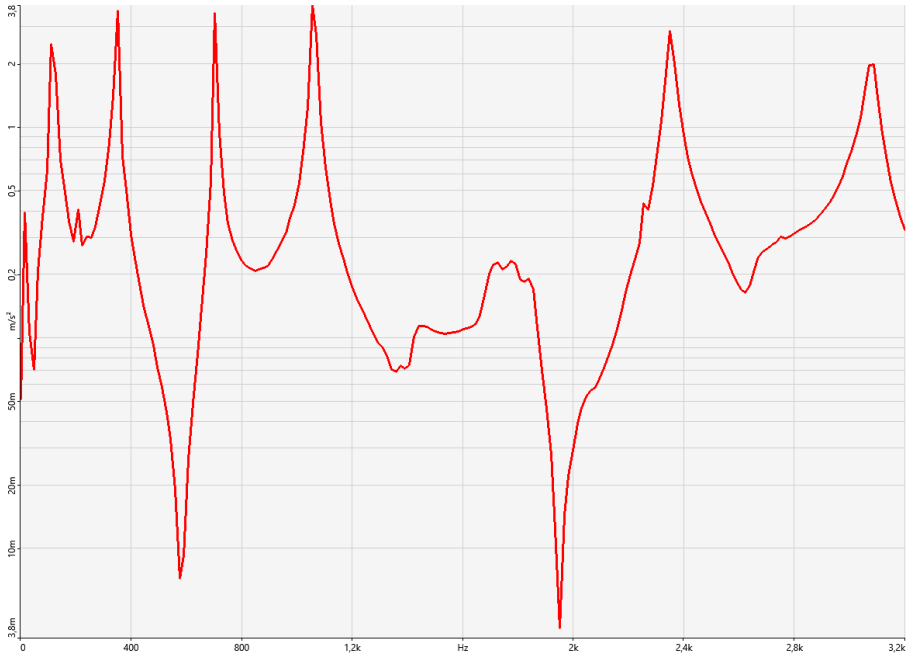


Figure A.III - 3: Frequency Response Function for S_G45_Si

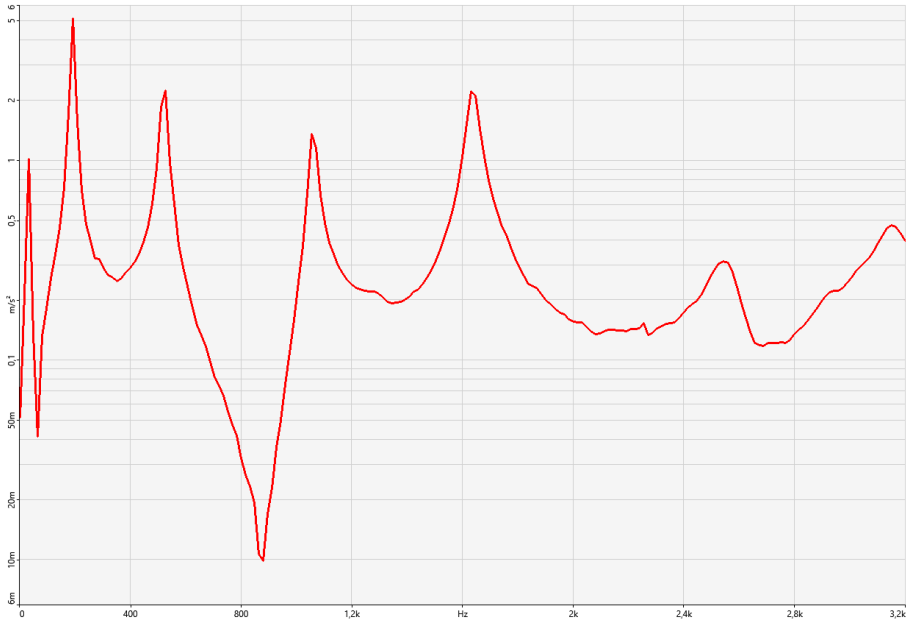


Figure A.III - 4: Frequency Response Function for S_G45_Ak

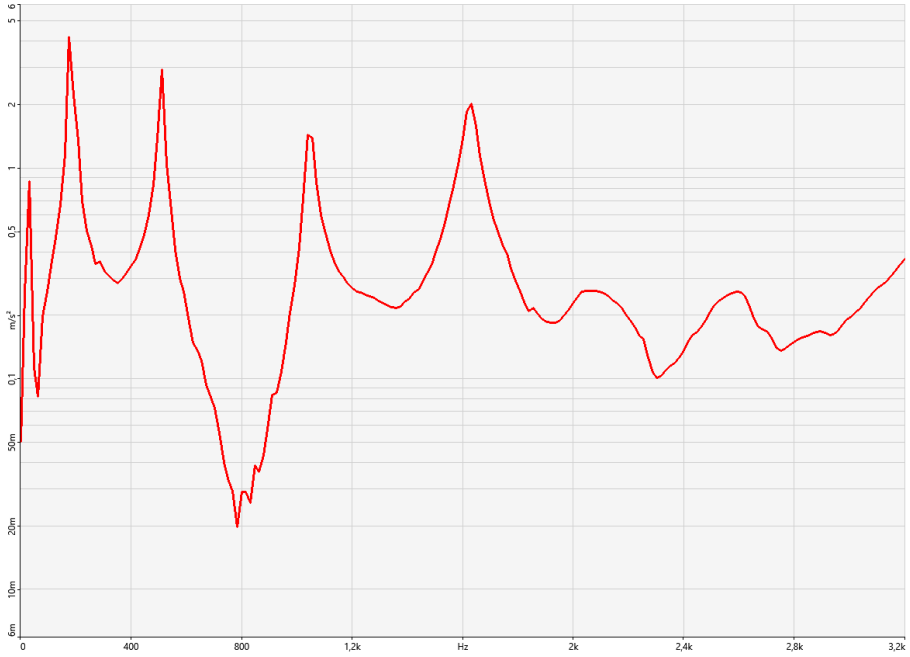
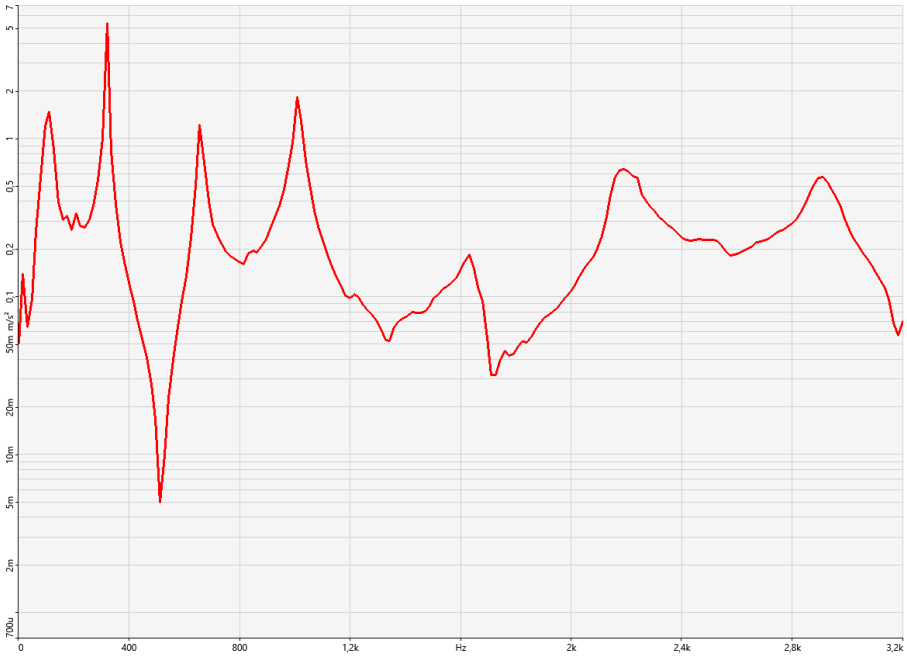


Figure A.III - 5: Frequency Response Function for S_F00_Si



THIS PAGE WAS INTENTIONALLY LEFT BLANK

APPENDIX IV: MODAL SHAPES

The following images represent the modal shapes obtained by experimental testing (using B&K Connect) for the probe S1_G45_Ak. The 5 triangle peaks represent the maximum displacement of the sensor at the different positions placed, [100; 120; 140; 160; 180]mm from the fixed end.

Figure A.IV - 1: Experimental test first modal shape for S1_G45_Ak

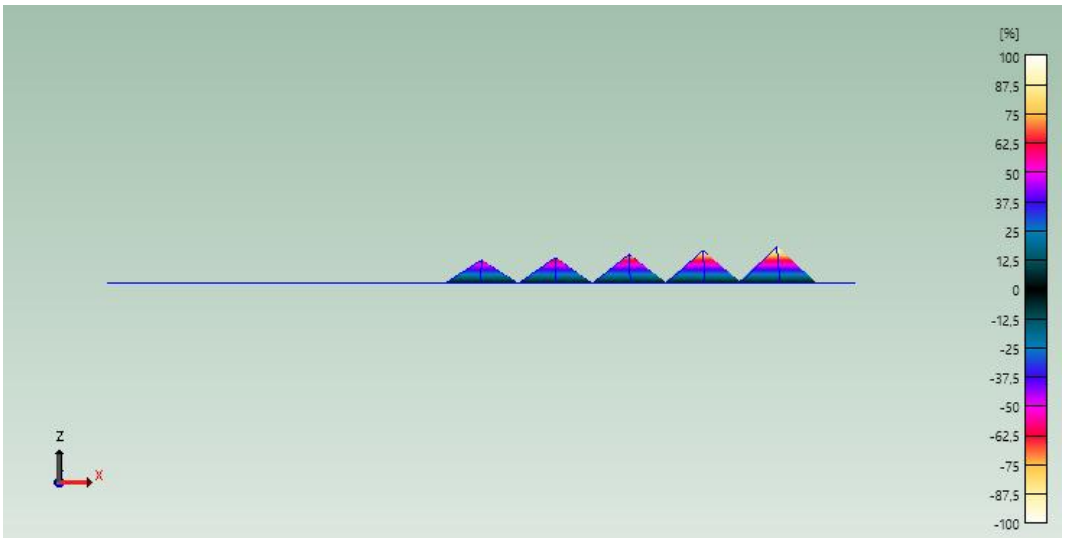


Figure A.IV - 2: Experimental test second modal shape for S1_G45_Ak

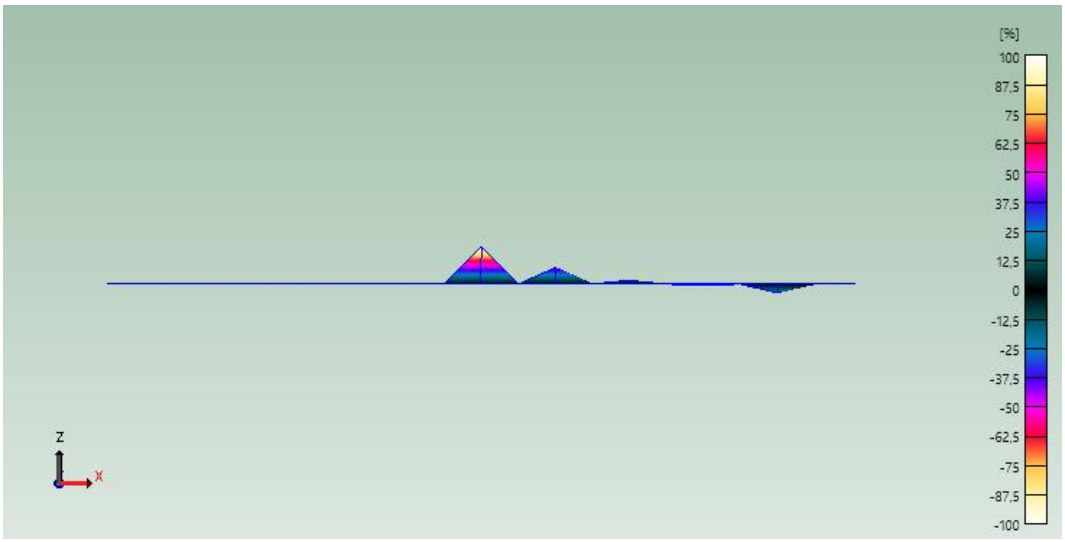


Figure A.IV - 3: Experimental test third modal shape for S1_G45_Ak

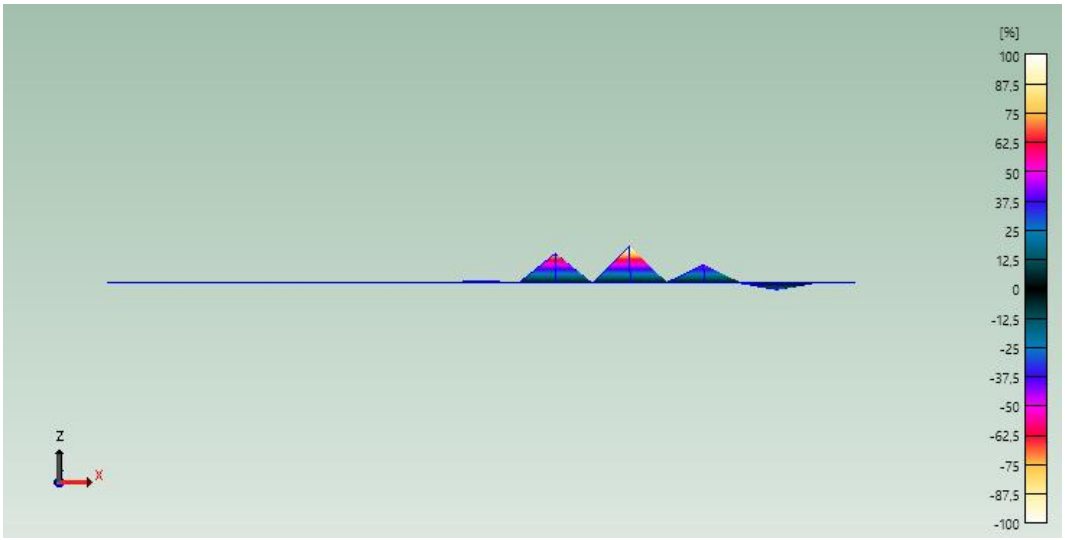


Figure A.IV - 4: Experimental test fourth modal shape for S1_G45_Ak

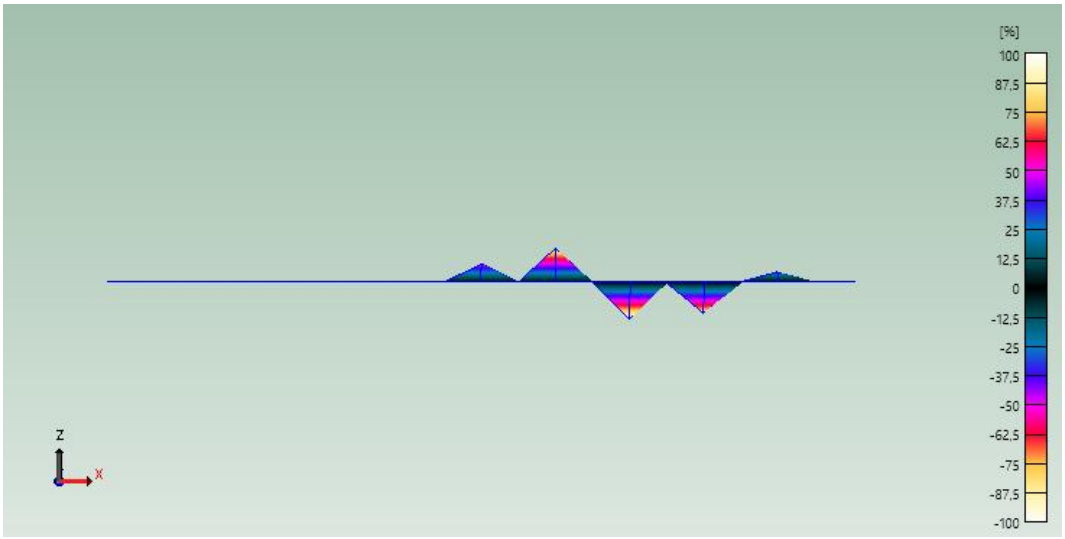


Figure A.IV - 5: Experimental test fifth modal shape for S1_G45_Ak

